PM6675S

High efficiency step-down controller with embedded 2 A LDO regulator

Features

- Switching section
  - 4.5 V to 28 V input voltage range
  - 0.6 V, ±1 % voltage reference
  - Selectable 1.5 V fixed output voltage
  - Adjustable 0.6 V to 3.3 V output voltage
  - 1.237 V ±1 % reference voltage available
  - Very fast load transient response using constant on-time control loop
  - No R_{SENSE} current sensing using low side MOSFETs' $R_{DS(ON)}$
  - Negative current limit
  - Latched OVP and UVP
  - Soft-start internally fixed at 3 ms
  - Selectable pulse skipping at light load
  - Selectable No-Audible (33 kHz) pulse skip mode
  - Ceramic output capacitors supported
  - Output voltage ripple compensation
  - Output soft-end
- LDO regulator section
  - Adjustable 0.6 V to 3.3 V output voltage
  - Selectable ±1 Apk or ±2 Apk current limit
  - Dedicated power-good signal
  - Ceramic output capacitors supported
  - Output soft-end

Applications

- Notebook computers
- Graphic cards
- Embedded computers

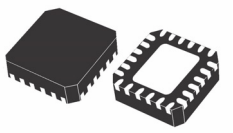

VFQFPN-24 4x4

Description

The PM6675S device consists of a single high efficiency step-down controller and an independent Low Drop-Out (LDO) linear regulator.

The Constant On-Time (COT) architecture assures fast transient response supporting both electrolytic and ceramic output capacitors. An embedded integrator control loop compensates the DC voltage error due to the output ripple.

A selectable low-consumption mode allows the highest efficiency over a wide range of load conditions. The low-noise mode sets the minimum switching frequency to 33 kHz for audio-sensitive applications.

The LDO linear regulator can sink and source up to 2 Apk. Two fixed current limits (±1 A-±2 A) can be chosen.

An active soft-end is independently performed on both the switching and the linear regulators outputs when disabled.

Table 1. Device summary

Order codes	Package	Packaging
PM6675S	VFQFPN-24 4x4 (exposed pad)	Tube
PM6675STR		Tape and reel

Contents

1 Typical application circuit

Figure 1. Application circuit

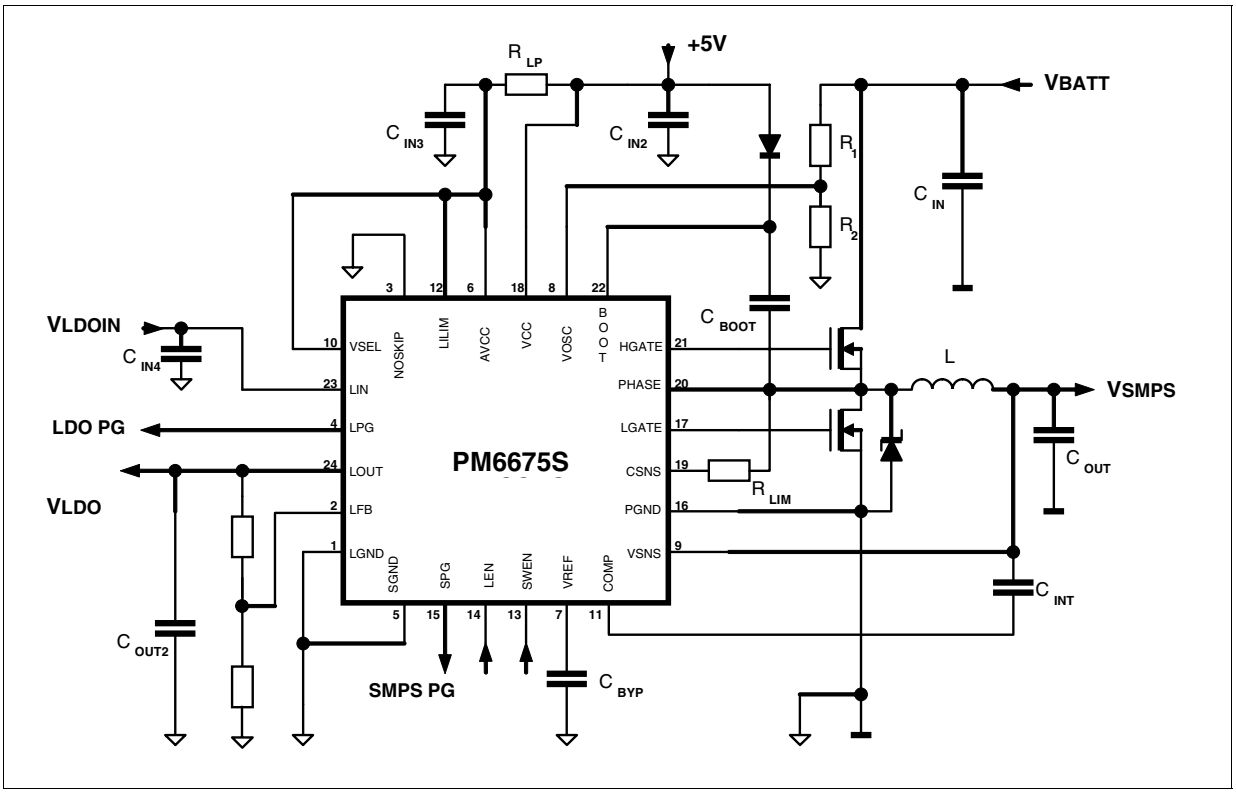

2 Pin settings

2.1 Connections

Figure 2. Pin connection (through top view)

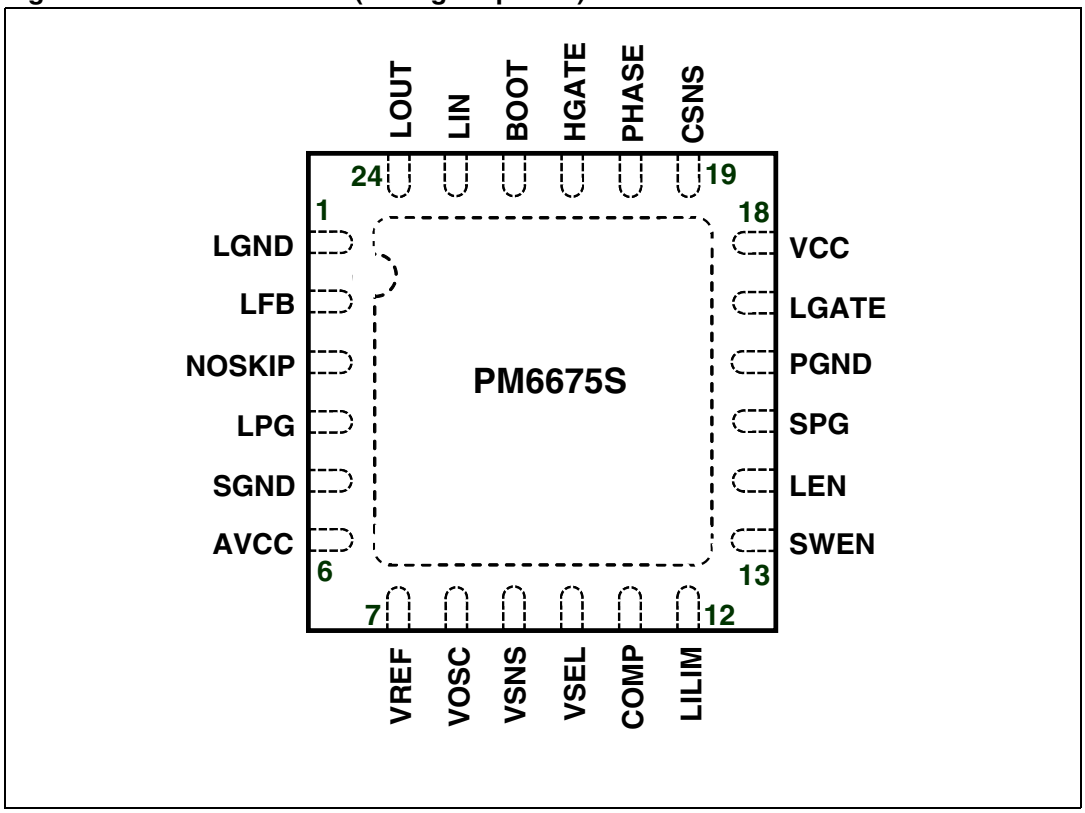

2.2 Pin description

Table 2. Pin functions

N°	Pin	Function
1	LGND	LDO power ground. Connect to the negative terminal of VTT output capacitor.
2	LFB	LDO remote sensing. Connect as close as possible to the load via a low noise PCB trace.
3	NOSKIP	Pulse-Skip/No-Audible Pulse-Skip Modes selector. See *Section 7.1.4: Mode-of-operation selection on page 30*
4	LPG	LDO section power-good signal (open drain output). High when LDO output voltage is within ±10 % of nominal value.
5	SGND	Ground reference for analog circuitry, control logic and VTTREF buffer. Connect together with the thermal pad and VTTGND to a low impedance ground plane. See the *Application Note* for details.
6	AVCC	+5 V supply for internal logic. Connect to +5 V rail through a simple RC filtering network.
7	VREF	High accuracy output voltage reference (1.237 V) for multilevel pins setting. It can deliver up to 50 µA. Connect a 100 nF capacitor between VREF and SGND in order to enhance noise rejection.
8	VOSC	Frequency selection. Connect to the central tap of a resistor divider to set the desired switching frequency. The pin cannot be left floating. See *Section 7: Device description on page 19* for details.
9	VSNS	Switching section output remote sensing and discharge path during output soft-end. Connect as close as possible to the load via a low noise PCB trace.
10	VSEL	Fixed output selector and feedback input for the switching controller. If VSEL pin voltage is higher than 4 V, the fixed 1.5 V output is selected. If VSEL pin voltage is lower than 4 V, it is used as negative input of the error amplifier. See *Section 7.1.4: Mode-of-operation selection on page 30* for details.
11	COMP	DC voltage error compensation input pin for the switching section. Refer to *Section 7.1.4: Mode-of-operation selection on page 30* for more details.
12	LILIM	Current limit selector for the LDO. Connect to SGND for ±1 A current limit or to +5 V for ±2 A current limit.
13	SWEN	Switching controller enable. When tied to ground, the switching output is turned off and a soft-end is performed.
14	LEN	Linear regulator enable. When tied to ground, the LDO output is turned off and a soft-end is performed.
15	SPG	Switching section power good signal (open drain output). High when the switching regulator output voltage is within ±10 % of nominal value.
16	PGND	Power ground for the switching section.
17	LGATE	Low-side gate driver output.
18	VCC	+5 V low-side gate driver supply. Bypass with a 100 nF capacitor to PGND.

Table 2. Pin functions (continued)

N°	Pin	Function
19	CSNS	Current sense input for the switching section. This pin must be connected through a resistor to the drain of the synchronous rectifier ($R_{DS(ON)}$ sensing) to set the current limit threshold.
20	PHASE	Switch node connection and return path for the high side gate driver.
21	HGATE	High-Side Gate Driver Output
22	BOOT	Bootstrap capacitor connection. Input for the supply voltage of the high-side gate driver.
23	LIN	Linear Regulator Input. Bypass to LGND by a 10µF ceramic capacitor for noise rejection enhancement.
24	LOUT	LDO linear regulator output. Bypass with a 20µF (2 x 10 µF MLCC) filter capacitor.

3 Electrical data

3.1 Maximum rating

Table 3. Absolute maximum ratings (1)

Symbol	Parameter	Value	Unit
V_{AVCC}	AVCC to SGND	-0.3 to 6	V
V_{VCC}	VCC to SGND	-0.3 to 6	
	PGND, LGND to SGND	-0.3 to 0.3	
	HGATE and BOOT to PHASE	-0.3 to 6	
	HGATE and BOOT to PGND	-0.3 to 44	
V_{PHASE}	PHASE to SGND	-0.3 to 38	
	LGATE to PGND	-0.3 to V_{CC} +0.3	
	CSNS, SPG, LEN, SWEN, LILIM, COMP, VSEL, VSNS, VOSC, VREF, NOSKIP to SGND	-0.3 to V_{AVCC} + 0.3	
	LPG,VREF, LOUT, LFB to SGND	-0.3 to V_{AVCC} + 0.3	
	LIN, LOUT, LPG, LIN to LGND	-0.3 to V_{AVCC} + 0.3	
	Maximum withstanding Voltage range test condition: CDF-AEC-Q100-002- “Human Body Model” acceptance criteria: “Normal Performance”	± 1250	V

1. Free air operating conditions unless otherwise specified. Stresses beyond those listed under "absolute maximum ratings" may cause permanent damage to the device. Exposure to absolute maximum rated conditions for extended periods may affect device reliability.

3.2 Thermal data

Table 4. Thermal data

Symbol	Parameter	Value	Unit
R_{thJA}	Thermal resistance junction to ambient	42	°C/W
T_{STG}	Storage temperature range	- 50 to 150	°C
T_A	Operating ambient temperature range	- 40 to 85	°C
T_J	Junction operating temperature range	- 40 to 125	°C

3.3 Recommended operating conditions

Table 5. Recommended operating conditions

Symbol	Parameter	Values			Unit
		Min	Typ	Max	
V_{IN}	Input voltage range	4.5		28	V
V_{AVCC}	IC supply voltage	4.5		5.5	
V_{VCC}	IC supply voltage	4.5		5.5	

4 Electrical characteristics

Table 6. Electrical characteristics

T_A = 0 °C to 85 °C, VCC = AVCC = +5 V, LIN = 1.5 V and LOUT = 0.6 V, if not otherwise specified (1)

Symbol	Parameter	Test condition		Values			Unit
				Min	Typ	Max	
Supply section							
I_{IN}	Operating current (Switching + LDO)	SWEN, LEN, VSEL and NOSKIP connected to AVCC, No load on LOUT output.				2	mA
I_{SW}	Operating current (Switching)	SWEN, VSEL and NOSKIP connected to AVCC, LEN connected to SGND.				1	
I_{SHDN}	Shutdown operating current	SWEN and LEN tied to SGND.				10	µA
UVLO	AVCC under voltage lockout upper threshold			4.1	4.25	4.4	V
	AVCC under voltage lockout upper threshold			3.85	4.0	4.1	
	UVLO hysteresis			70			mV
ON-time (SMPS)							
t_{ON}	On-time duration	VSEL low, NOSKIP low, V_{VSNS} = 2V	VOSC=300 mV	530	630	730	ns
			VOSC=500 mV	320	380	440	
OFF-time (SMPS)							
t_{OFFMIN}	Minimum OFF-time				300	350	ns
Voltage reference							
	Voltage accuracy	4.5 V< V_{IN} < 25 V		1.224	1.237	1.249	V
	Load regulation	-50 µA< I_{VREF} < 50 µA		-4		4	mV
	Undervoltage Lockout Fault Threshold				800		

Table 6. Electrical characteristics (continued)
T_A = 0 °C to 85 °C, VCC = AVCC = +5 V, LIN = 1.5 V and LOUT = 0.6 V, if not otherwise specified (1)

Symbol	Parameter	Test condition	Values			Unit
			Min	Typ	Max	
SMPS output						
V_{OUT}	SMPS fixed output voltage	VSEL connected to AVCC, NOSKIP tied to SGND, No Load		1.5		V
	Feedback output voltage accuracy		-1.5		1.5	%
Current limit and zero crossing comparator						
I_{CSNS}	CSNS input bias current		90	100	110	µA
	Comparator offset		-6		6	mV
	Positive current limit threshold	V_{PGND} - V_{CSNS}		100		
	Fixed negative current limit threshold			110		
$V_{ZC,OFFS}$	Zero crossing comparator offset		-11	-5	1	
High and low side gate drivers						
	HGATE driver on-resistance	HGATE high state (pull-up)		2.0	3	Ω
		HGATE low state (pull-down)		1.8	2.7	
	LGATE driver on-resistance	LGATE high state (pull-up)		1.4	2.1	
		LGATE low state (pull-down)		0.6	0.9	
UVP/OVP protections and PGOOD signals						
OVP	Over voltage threshold		112	115	118	%
UVP	Under voltage threshold		67	70	73	
PGOOD	SMPS upper threshold		107	110	113	
	SMPS lower threshold		86	90	93	
	LDO upper threshold		107	110	113	
	LDO lower threshold		86	90	93	
$I_{PG,LEAK}$	SPG and LPG Leakage Current	SPG and LPG forced to 5.5 V			1	µA
$V_{PG,LOW}$	SPG and LPG Low Level Voltage	$I_{LPG,SINK}$ = $I_{SPG,SINK}$ = 4 mA		150	250	mV
Soft-start section (SMPS)						
	Soft-start ramp time (4 steps current limit)		2	3	4	ms
	Soft-start current limit step			25		µA

Table 6. Electrical characteristics (continued)
T_A = 0 °C to 85 °C, VCC = AVCC = +5 V, LIN = 1.5 V and LOUT = 0.6 V, if not otherwise specified (1)

Symbol	Parameter	Test condition	Values			Unit
			Min	Typ	Max	
Soft-end section						
	Switching section discharge resistance		15	25	35	Ω
	LDO section discharge resistance		15	25	35	
LDO section						
V_{LREF}	LDO reference voltage			600		mV
	LDO output accuracy respect to VREF	-1 mA < I_{LDO} < 1 mA	-20		20	
		-1 A < I_{LDO} < 1 A	-25		25	
$I_{LDO,CL}$	LDO sink current limit	V_{LFB} > V_{LREF} , LILIM = 5 V	-3	-2.3	-2	A
		V_{LFB} > V_{LREF}, LILIM = 0 V	-1.6	-1.3	-1	
	LDO source current limit	0.9 • V_{LREF} < V_{LFB} < V_{LREF}, LILIM = 5V	2	2.4	3	
		0.9 • V_{LREF} < V_{LFB} < V_{LREF}, LILIM = 0V	1	1.3	1.6	
		V_{LFB} < 0.9 • V_{LREF}, LILIM = 5 V	1	1.3	1.6	
		V_{LFB} < 0.9 • V_{LREF}, LILIM = 0 V	0.5	0.8	1.1	
$I_{LIN,BIAS}$	LDO input bias current, ON	LEN connected to AVCC, no load		1	10	µA
	LDO input bias current, OFF	LEN = 0 V, no load			1	
$I_{LFB,BIAS}$	LFB input bias current	LEN connected to AVCC V_{LFB} = 0.6 V	-1		1	
$I_{LFB,LEAK}$	LFB leakage current	LEN = 0 V, V_{LFB} = 0.6 V	-1		1	

Table 6. Electrical characteristics (continued)

T_A = 0 °C to 85 °C, VCC = AVCC = +5 V, LIN = 1.5 V and LOUT = 0.6 V, if not otherwise specified (1)

Symbol	Parameter	Test condition	Values			Unit
			Min	Typ	Max	
Power management section						
$V_{VTHVSEL}$	VSEL pin thresholds	Fixed mode	V_{AVCC} -0.7			V
		Adjustable mode			V_{AVCC} -1.3	
$V_{VTHNOSKIP}$	NOSKIP pin thresholds	Forced-PWM mode	V_{AVCC} -0.8			
		No-audible mode	1.0		V_{AVCC} -1.5	
		Pulse-skip mode			0.5	
V_{VTHLEN}, $V_{VTHSWEN}$	LEN, SWEN turn off level		0.4			
	LEN, SWEN turn on level				1.6	
$V_{VTHLILIM}$	LILIM pin thresholds	±2 A LDO current limit	V_{AVCC} -0.8			
		±1 A LDO current limit			0.5	
$I_{IN,LEAK}$	Logic input leakage current	LEN, SWEN and LILIM = 5 V			10	µA
$I_{IN3,LEAK}$	Multilevel input leakage current	VSEL and NOSKIP = 5 V			10	
$I_{OSC,LEAK}$	VOSC pin leakage current	VOSC = 1 V			1	
Thermal shutdown						
T_{SHDN}	Shutdown temperature (2)			150		°C

1. $T_A = T_J$. All parameters at operating temperature extremes are guaranteed by design and statistical analysis (not production tested)
2. Guaranteed by design. Not production tested.

5 Typical operating characteristics

Figure 3. VOUT efficiency vs load, 1.5 V, SW frequency = 400 kHz

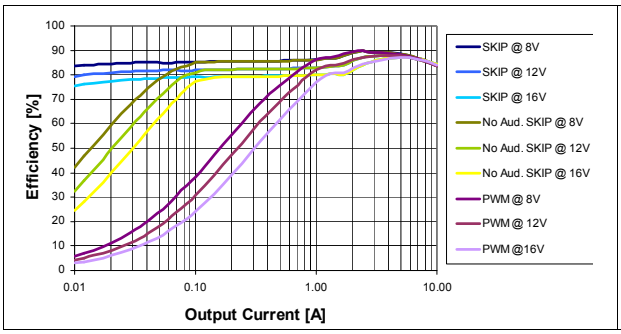

Figure 4. VOUT efficiency vs load, 1.25 V, SW frequency = 400 kHz

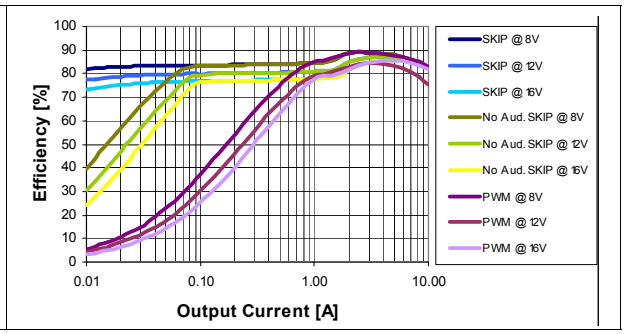

Figure 5. VOUT load regulation, 1.5 V, Vin = 12 V

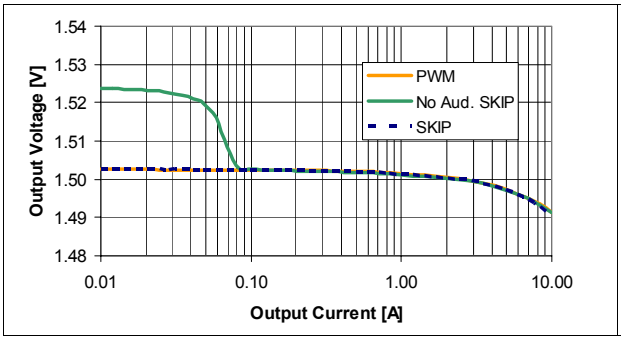

Figure 6. VOUT load regulation, 1.25 V, Vin = 12 V

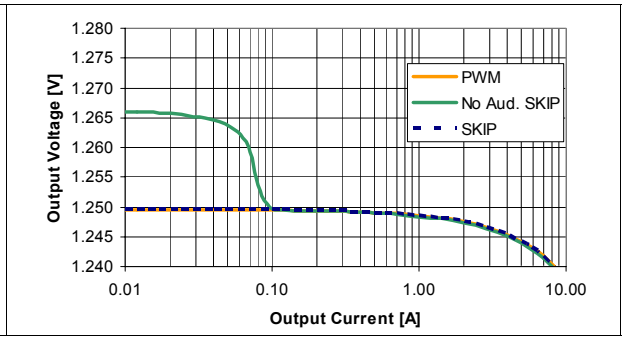

Figure 7. VOUT load regulation, 2.5 V, Vin = 12 V

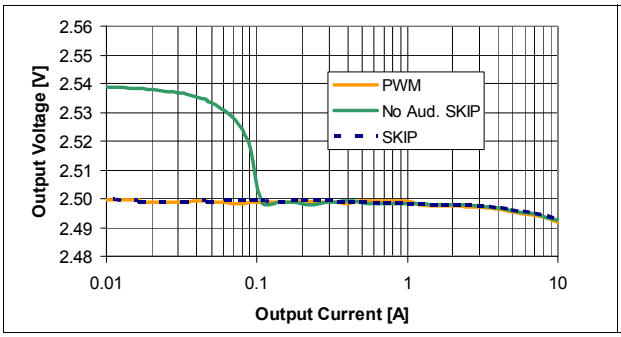

Figure 8. LOUT load regulation, LOUT = 0.9 V, LIN = 1.5 V

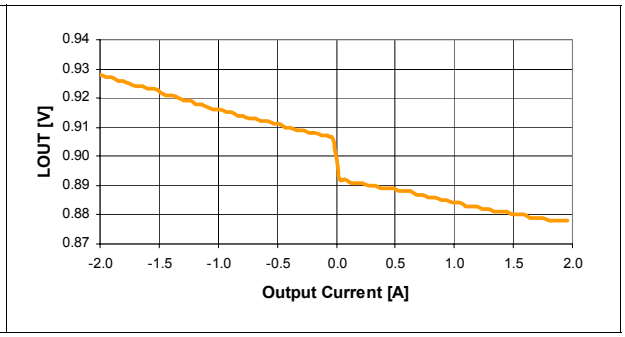

Figure 9. VOUT line regulation, 1.5 V, 0 A

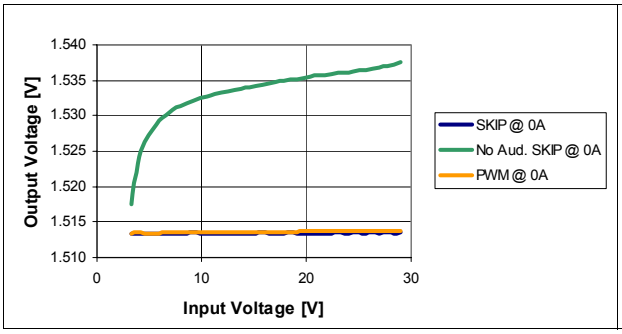

Figure 10. VOUT line regulation, 1.25 V, 0 A

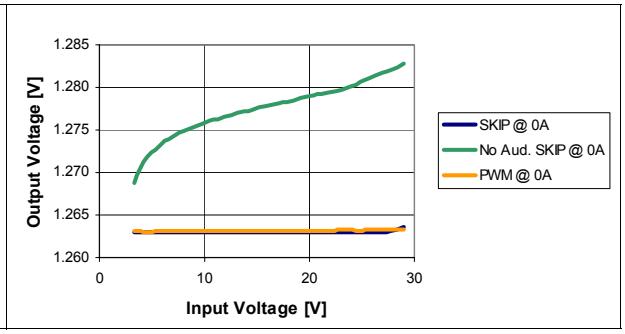

Figure 11. VOUT line regulation, 1.5 V

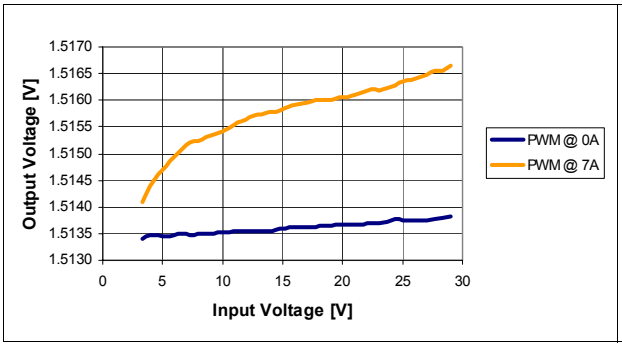

Figure 12. VOUT line regulation, 1.25 V

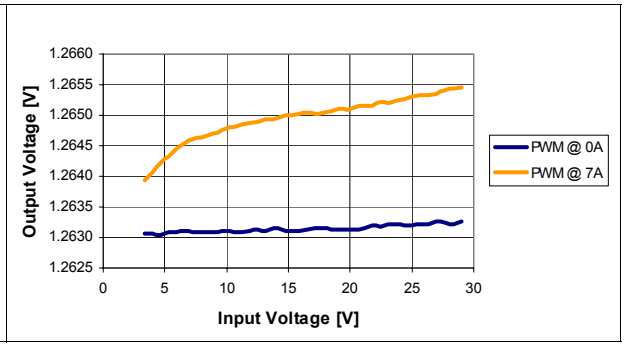

Figure 13. Switching frequency vs input voltage, 1.5 V

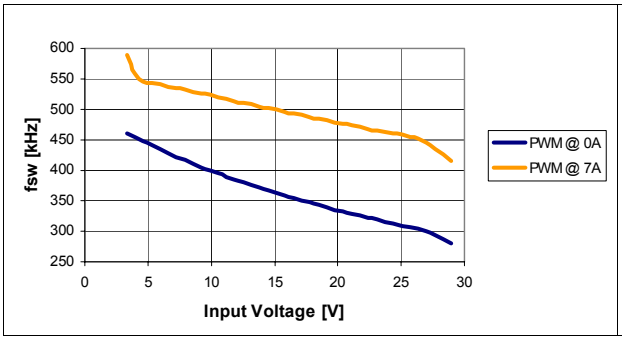

Figure 14. Switching frequency vs input voltage, 1.25 V

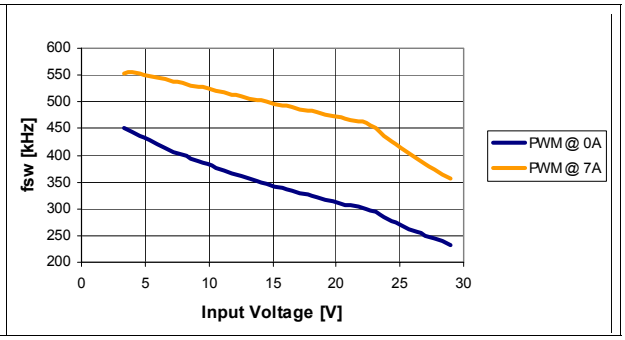

Figure 15. Switching frequency vs load - 1.5 V

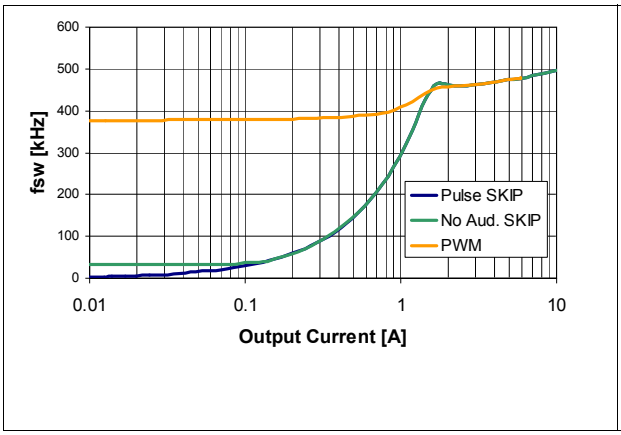

Figure 16. PWM waveforms

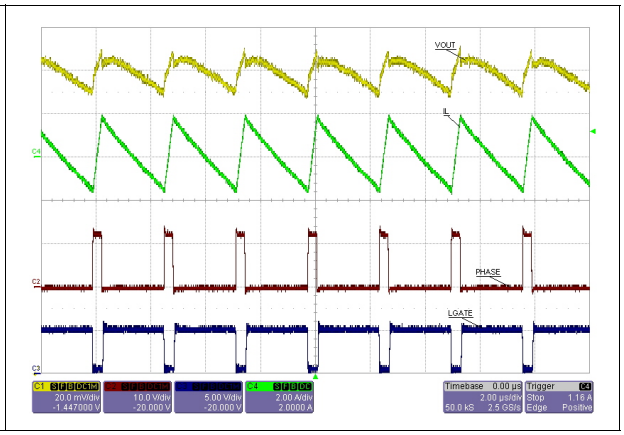

Figure 17. No-audible pulse-skip waveforms

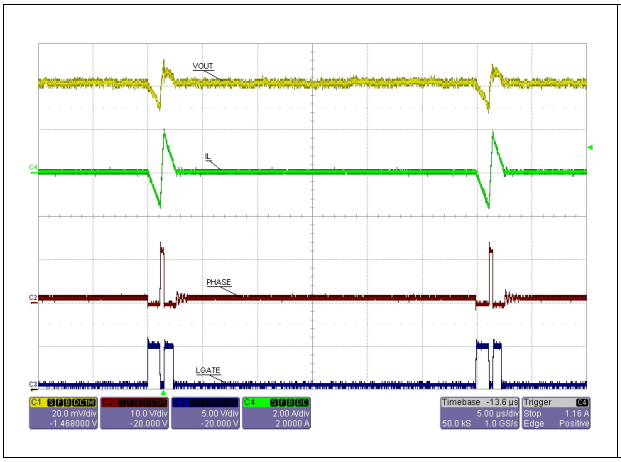

Figure 18. Pulse-skip waveforms

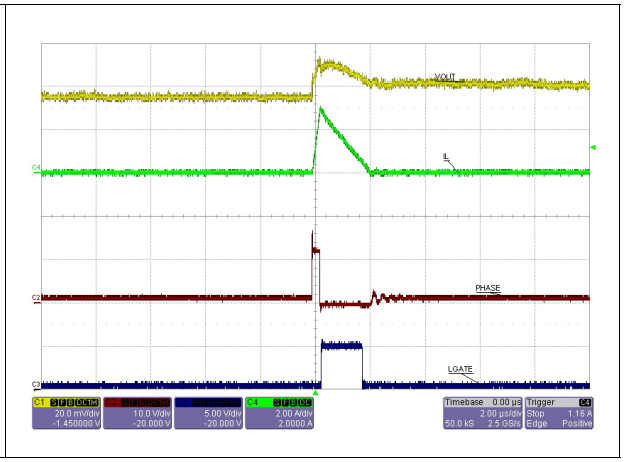

Figure 19. Power-up sequence VCC above UVLO

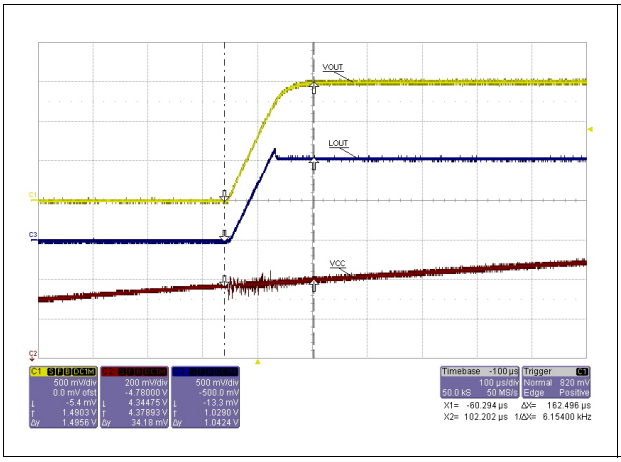

Figure 20. VOUT soft-start, 1.5 V, heavy load

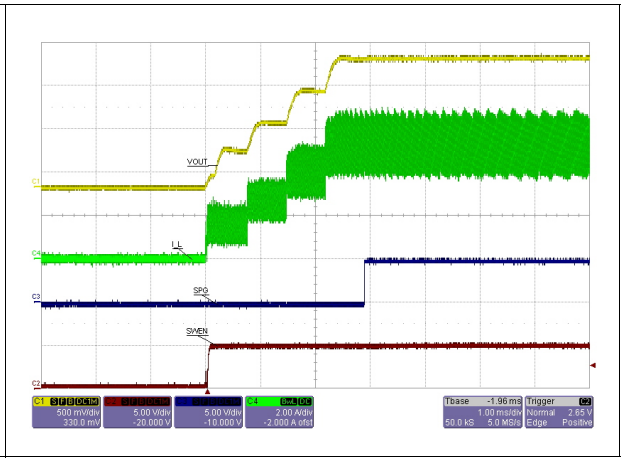

Figure 21. Switching section output soft-end

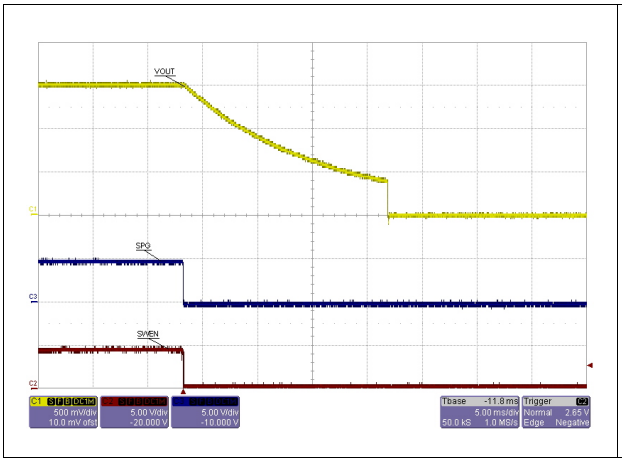

Figure 22. LDO section output soft-end

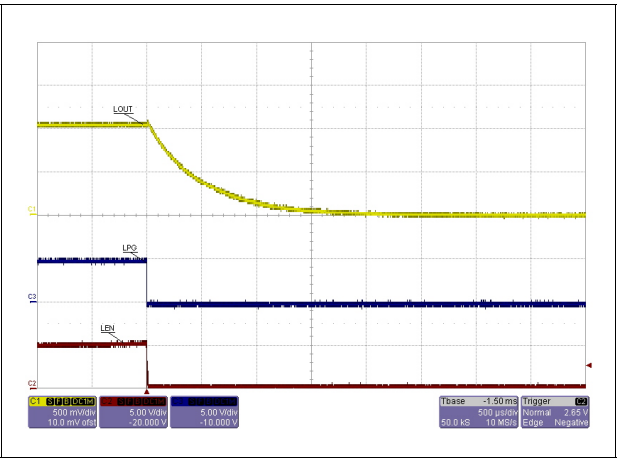

Figure 23. -1.8 A to 1.8 A LOUT load transient, 0.9 V

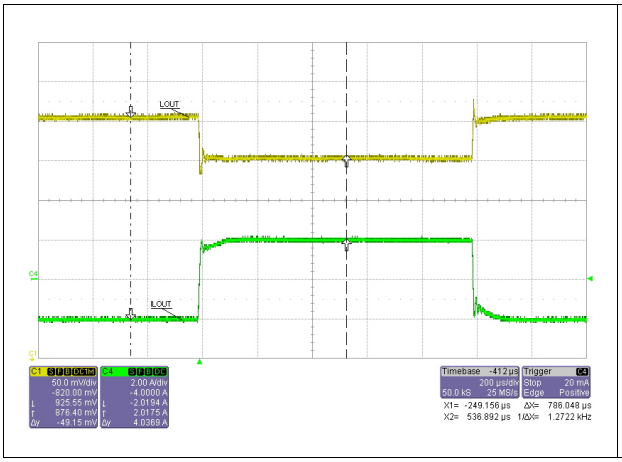

Figure 24. -1 A to 1 A LOUT load transient, 0.9 V

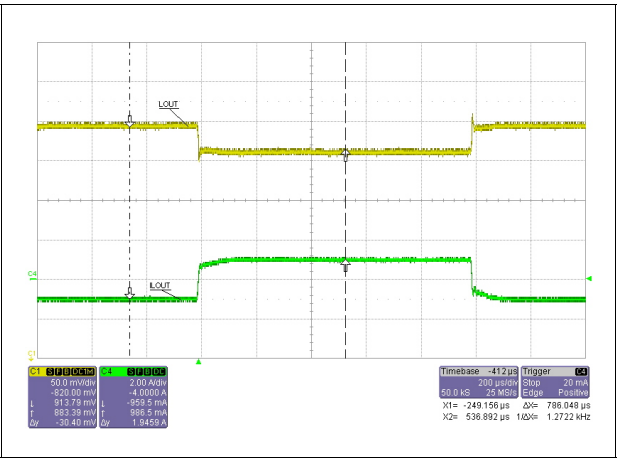

Figure 25. 0 A to 8 A VOUT load transient, PWM

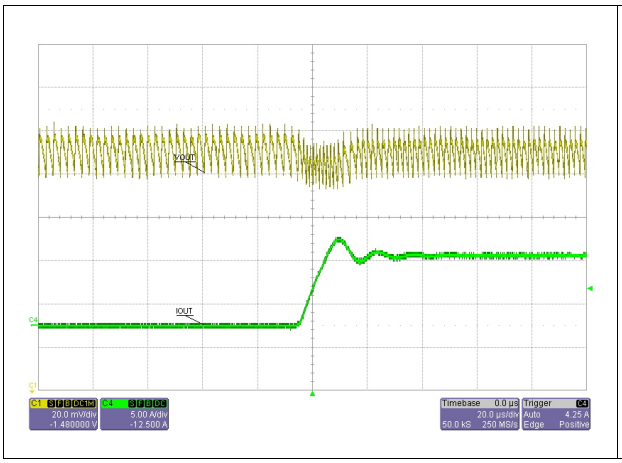

Figure 26. 8 A to 0 A VOUT load transient, PWM

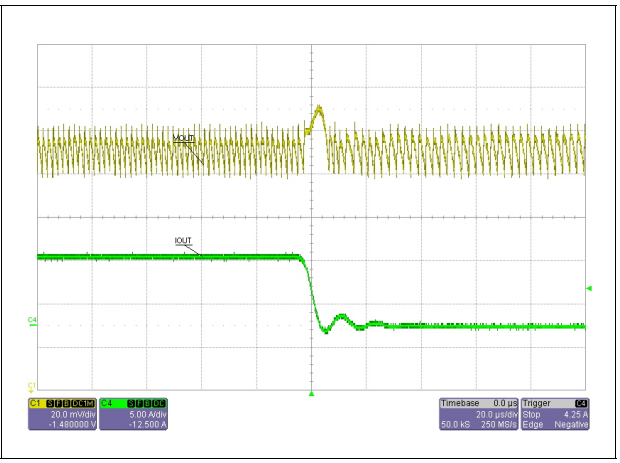

Figure 27. 0 A to 5 A VOUT load transient, Pulse-Skip

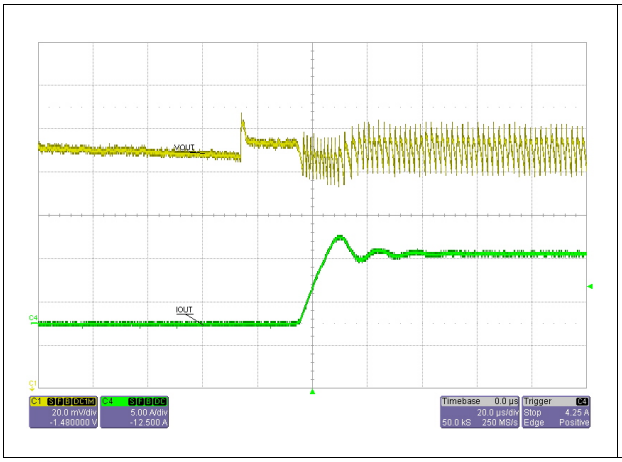

Figure 28. 5 A to 0 A VOUT load transient, Pulse-Skip

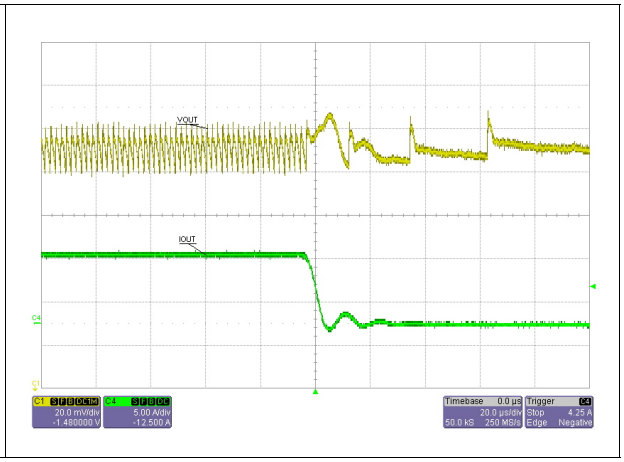

Figure 29. Over-voltage protection, VOUT = 1.5 V

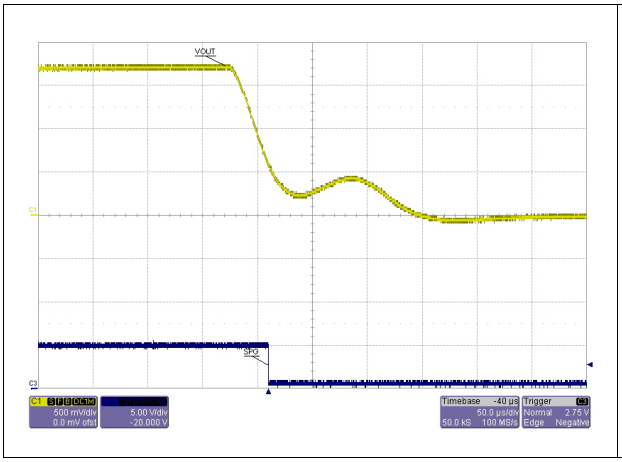

Figure 30. Under-voltage protection, VOUT = 1.5 V

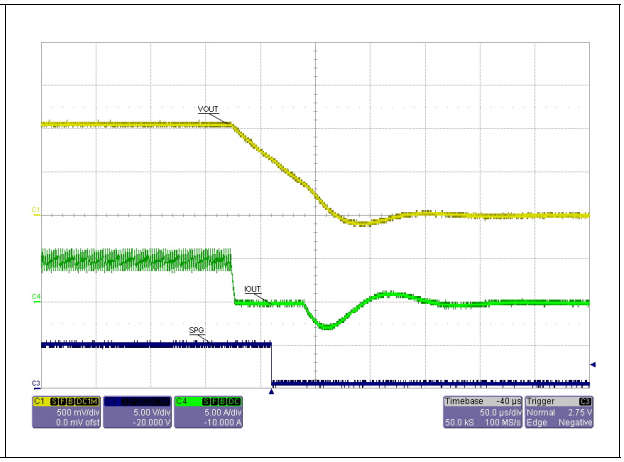

6 Block diagram

Figure 31. Functional and block diagram

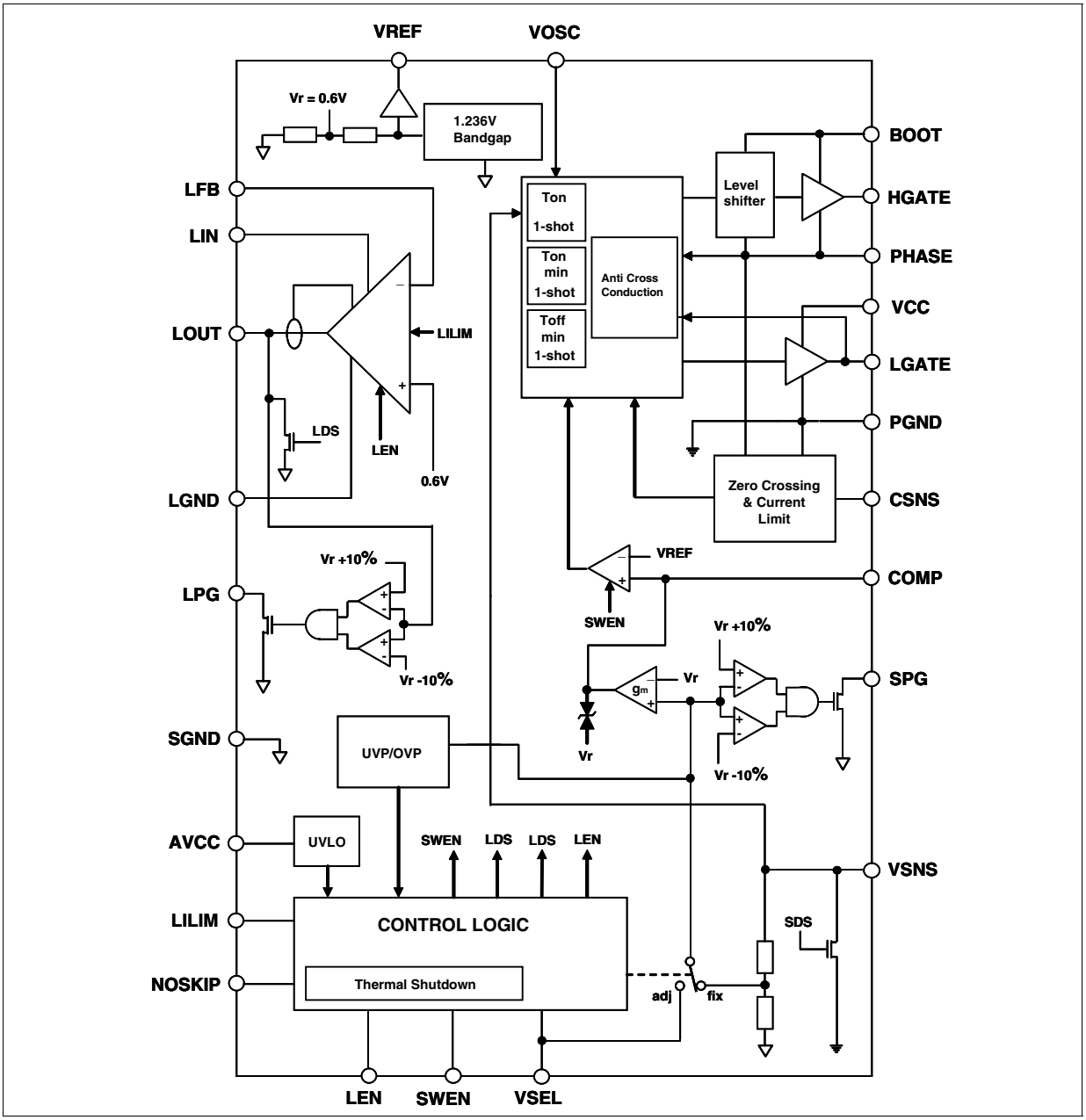

Table 7. Legend

SWEN	Switching controller enable
LEN	LDO regulator enable
LDS	LDO output discharge enable
SDS	Switching output discharge enable
LILIM	LDO regulator current limit

7 Device description

The PM6675S combines a single high efficiency step-down controller and an independent Low Drop-Out (LDO) linear regulator in the same package.

The switching controller section is a high-performance, pseudo-fixed frequency, Constant-On-Time (COT) based regulator specifically designed for handling fast load transient over a wide range of input voltages.

The switching section output can be easily set to a fixed 1.5 V voltage without additional components or adjusted in the 0.6 V to 3.3 V range using an external resistor divider. The Switching Mode Power Supply (SMPS) can handle different modes of operation in order to minimize noise or power consumption, depending on the application needs. Selectable low-consumption and low-noise modes allow the highest efficiency and a 33 kHz minimum switching frequency respectively at light loads.

A lossless current sensing scheme, based on the Low-Side MOSFET turn-on resistance, avoids the need for an external sensing resistor.

The input of the LDO can be either the switching section output or a lower voltage rail in order to reduce the total power dissipation. Linear regulator stability is achieved by filtering its output with a ceramic capacitor (20 µF or greater). The LDO linear regulator can sink and source up to 2 Apk.
Two fixed current limit (±1 A-±2 A) can be chosen.

An active soft-end is independently performed on both the switching and the linear regulators outputs when disabled.

7.1 Switching section - constant on-time PWM controller

The PM6675S employes a pseudo-fixed frequency, Constant On-Time (COT) controller as the core of the switching section. It is well known that the COT controller uses a relatively simple algorithm and uses the ripple voltage derived across the output capacitor ESR to trigger the On-Time one-shot generator. In this way, the output capacitor ESR acts as a current sense resistor providing the appropriate ramp signal to the PWM comparator. Nearly constant switching frequency is achieved by the system loop in steady-state operating conditions by varying the On-Time duration, avoiding thus the need for a clock generator. The On-Time one shot duration is directly proportional to the output voltage, detected by theVSNS pin, and inversely proportional to the input voltage, detected by the the VOSC pin, as follows:

Equation 1

$$T_{ON} = K_{OSC} \frac{V_{SNS}}{V_{OSC}} + \tau$$

where K_{OSC} is a constant value (130 ns typ.) and τ is the internal propagation delay (40ns typ.). The one-shot generator directly drives the high-side MOSFET at the beginning of each switching cycle allowing the inductor current to increase; after the On-Time has expired, an Off-Time phase, in which the low-side MOSFET is turned on, follows. The Off-Time duration is solely determined by the output voltage: when lower than the set value (i.e. the voltage at VSNS pin is lower than the internal reference V_R = 0.6 V), the synchronous rectifier is turned off and a new cycle begins (*Figure 32*).

Figure 32. Inductor current and output voltage in steady state conditions

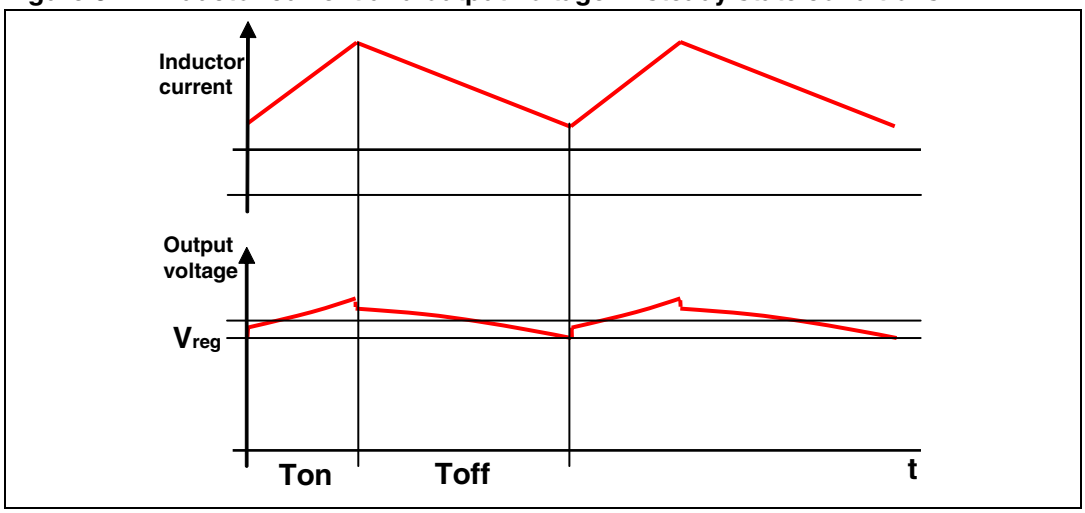

The duty-cycle of the buck converter is, in steady-state conditions, given by

Equation 2

$$D = \frac{V_{OUT}}{V_{IN}}$$

The switching frequency is thus calculated as

Equation 3

$$f_{SW} = \frac{D}{T_{ON}} = \frac{\frac{V_{OUT}}{V_{IN}}}{K_{OSC}\frac{V_{SNS}}{V_{OSC}}} = \frac{\alpha_{OSC}}{\alpha_{OUT}} \cdot \frac{1}{K_{OSC}}$$

where

Equation 4a

$$\alpha_{OSC} = \frac{V_{OSC}}{V_{IN}}$$

Equation 4b

$$\alpha_{OUT} = \frac{V_{SNS}}{V_{OUT}}$$

Referring to the typical application schematic (figures on cover page and *Figure 33*), the final expression is then:

Equation 5

$$f_{SW} = \frac{\alpha_{OSC}}{K_{OSC}} = \frac{R_2}{R_1 + R_2} \cdot \frac{1}{K_{OSC}}$$

Even if the switching frequency is theoretically independent from battery and output voltages, parasitic parameters involved in the power path (like MOSFET on-resistance and inductor DCR) introduce voltage drops responsible for a slight dependence on load current. In addition, the internal delay is due to a small dependence on input voltage.

The PM6675S switching frequency can be set by an external divider connected to the VOSC pin.

Figure 33. Switching frequency selection and VOSC pin

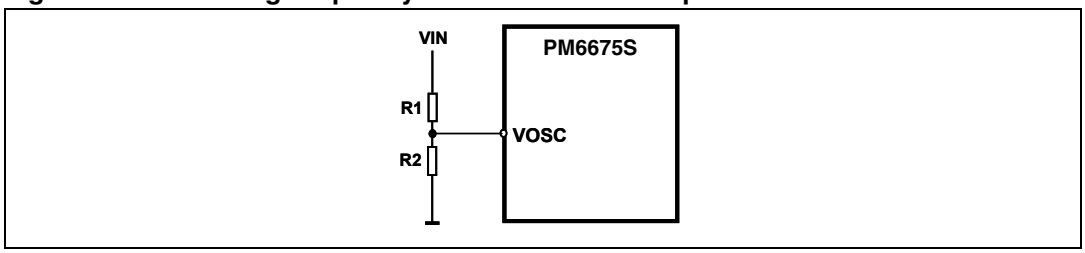

The voltage seen at this pin must be greater than 0.8 V and lower than 2 V in order to ensure the system linearity.

7.1.1 Constant-On-Time architecture

Figure 34 shows the simplified block diagram of the Constant-On-Time controller.

The switching regulator of the PM6675S controls a one-shot generator that turns on the high-side MOSFET when the following conditions are simultaneously satisfied: the PWM comparator is high (i.e. output voltage is lower than Vr = 0.6 V), the synchronous rectifier current is below the current limit threshold and the minimum off-time has expired.

A minimum Off-Time contraint (300ns typ.) is introduced to assure the boot capacitor charge and allow inductor valley current sensing on low-side MOSFET. A minimum On-Time is also introduced to assure the start-up switching sequence.

Once the On-Time has timed out, the high side switch is turned off, while the synchronous rectifier is ignited according to the anti-cross conduction management circuitry.

When the output voltage reaches the valley limit (determined by internal reference Vr = 0.6 V), the low-side MOSFET is turned off according to the anti-cross conduction logic once again, and a new cycle begins.

Figure 34. Switching section simplified block diagram

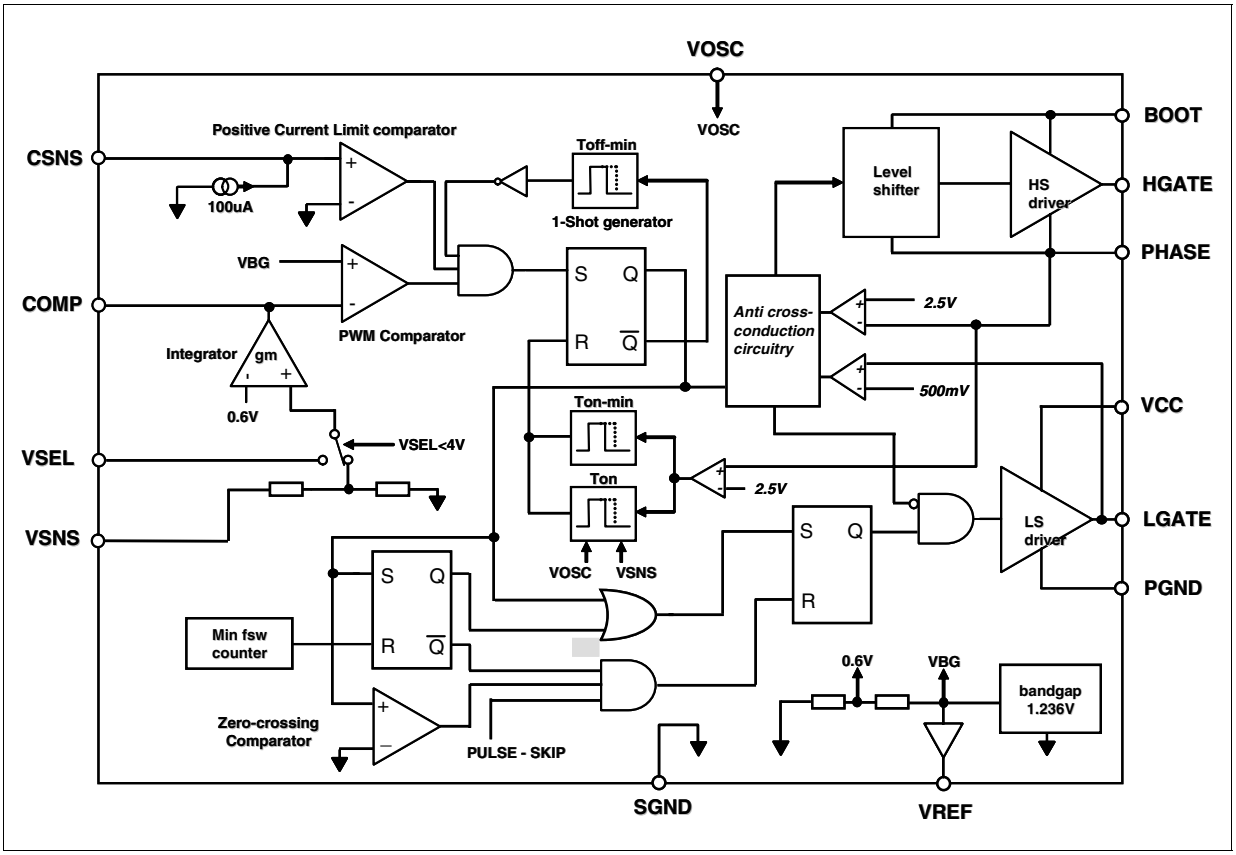

7.1.2 Output ripple compensation and loop stability

The loop is closed connecting the center tap of the output divider (internally, when the fixed output voltage is chosen, or externally, using the VSEL pin in the adjustable output voltage mode). The feedback node is the negative input of the error comparator, while the positive input is internally connected to the reference voltage (Vr = 0.6 V). When the feedback voltage becomes lower than the reference voltage, the PWM comparator goes to high and sets the control logic, turning on the high-side MOSFET. After the On-Time (calculated as previously described), the system releases the high-side MOSFET and turns on the synchronous rectifier.

The voltage drop along ground and supply PCB paths, used to connect the output capacitor to the load, is a source of DC error. Furthermore the system regulates the output voltage valley, not the average, as shown in *Figure 37*. Thus, the voltage ripple on the output capacitor is an additional source of DC error. To compensate this error, an integrative network is introduced in the control loop, by connecting the output voltage to the COMP pin through a capacitor (C_{INT}) as shown in *Figure 35*.

Figure 35. Circuitry for output ripple compensation

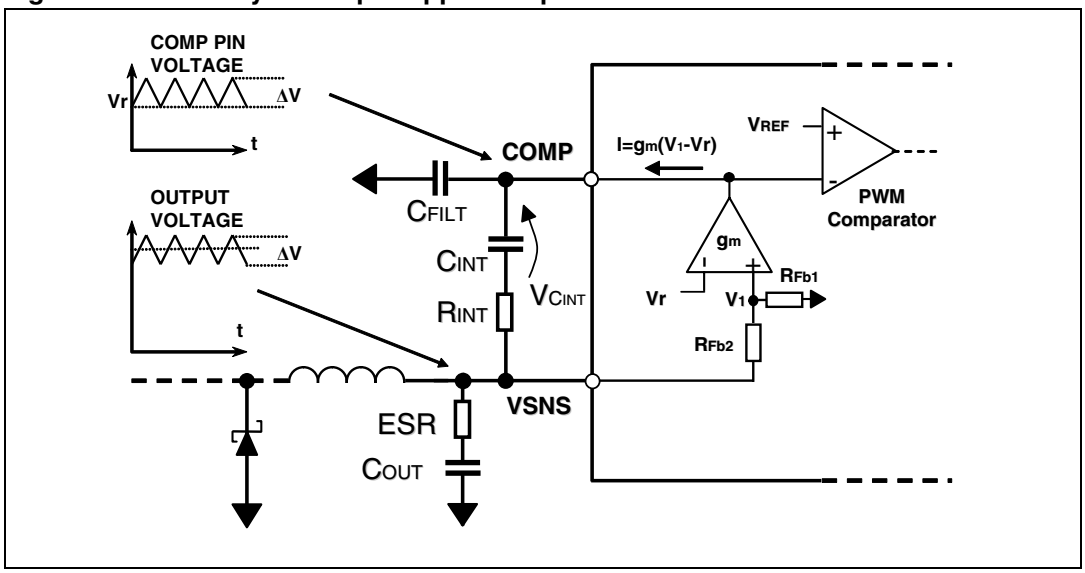

The additional capacitor is used to reduce the voltage on the COMP pin when higher than 300 mVpp and is unnecessary for most of applications. The trans conductance amplifier (gm) generates a current, proportional to the DC error, used to charge the C_{INT} capacitor. The voltage across the C_{INT} capacitor feeds the negative input of the PWM comparator, forcing the loop to compensate the total static error. An internal voltage clamp forces the COMP pin voltage range to ±150 mV respect to V_{REF}. This is useful to avoid or smooth output voltage overshoot during a load transient. When the Pulse-Skip Mode is entered, the clamping range is automatically reduced to 60 mV in order to enhance the recovering capability. If the ripple amplitude is larger than 150 mV, an additional capacitor C_{FILT} can be connected between the COMP pin and ground to reduce ripple amplitude, otherwise the integrator will operate out of its linearity range. This capacitor is unnecessary for most of applications and can be omitted.

The design of the external feedback network depends on the output voltage ripple. If the ripple is higher than approximately 20 mV, the correct C_{INT} capacitor is usually enough to keep the loop stable. The stability of the system depends firstly on the output capacitor zero frequency.

The following condition must be satisfied:

Equation 6

$$f_{SW} > k \cdot f_{Zout} = \frac{k}{2\pi \cdot C_{out} \cdot ESR}$$

where k is a fixed design parameter (k > 3). It determinates the minimum integrator capacitor value:

Equation 7

$$C_{INT} > \frac{g_m}{2\pi \cdot \left(\frac{f_{SW}}{k} - f_{Zout}\right)} \cdot \frac{Vr}{Vout}$$

where gm = 50 µs is the integrator trans conductance.

If the ripple on the COMP pin is greater than 150 mV, the auxiliary capacitor C_{FILT} can be added. If q is the desired attenuation factor of the output ripple, C_{FILT} is given by:

Equation 8

$$C_{FILT} = \frac{C_{INT} \cdot (1-q)}{q}$$

In order to reduce the noise on the COMP pin, it is possible to add a resistor R_{INT} that, together with CINT and C_{FILT}, becomes a low pass filter. The cutoff frequency f_{CUT} must be much greater (10 or more times) than the switching frequency:

Equation 9

$$R_{INT} = \frac{1}{2\pi \cdot f_{CUT} \cdot \frac{C_{INT} \cdot C_{FILT}}{C_{INT} + C_{FILT}}}$$

If the ripple is very small (lower than approximately 20mV), a different compensation network, called "Virtual-ESR" Network, is needed. This additional circuit generates a triangular ripple that is added to the output voltage ripple at the input of the integrator. The complete control scheme is shown in *Figure 36*.

Figure 36. "Virtual-ESR" network

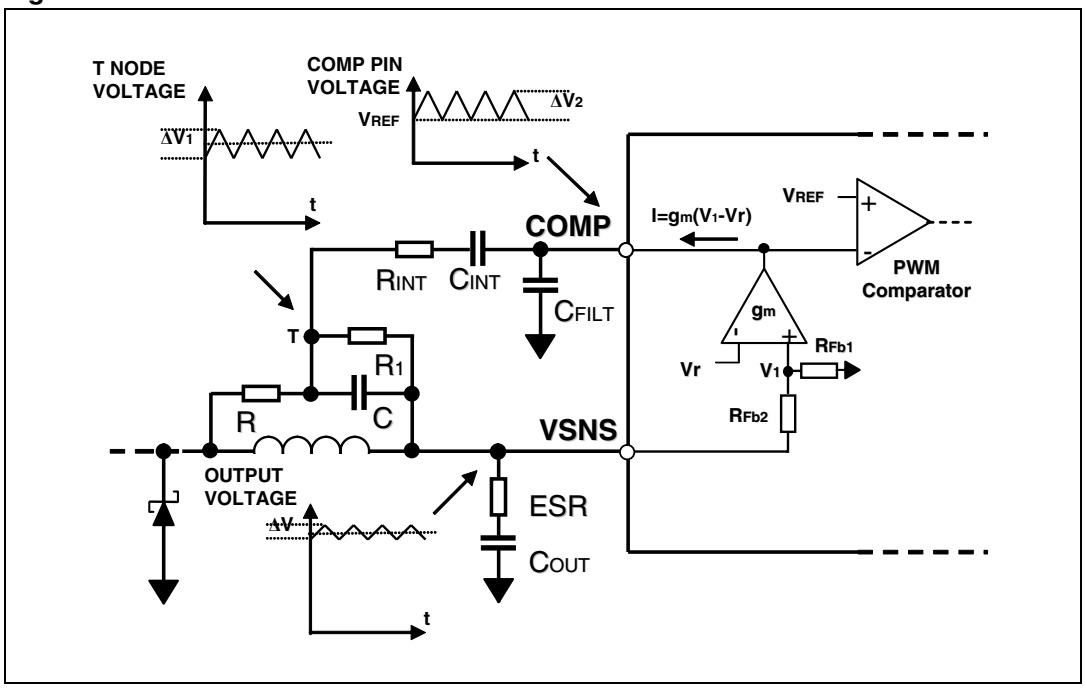

The ripple on the COMP pin is the sum of the output voltage ripple and the triangular ripple generated by the Virtual-ESR Network. In fact the Virtual-ESR Network behaves like a another equivalent series resistor R_{VESR}.

A good trade-off is to design the network in order to achieve an R_{VESR} given by:

Equation 10

$$R_{VESR} = \frac{V_{RIPPLE}}{\Delta I_L} - ESR$$

where ΔI_L is the inductor current ripple and V_{RIPPLE} is the total ripple at the T node, chosen greater than approximately 20 mV.

The new closed-loop gain depends on C_{INT}. In order to ensure stability it must be verified that:

Equation 11

$$C_{INT} > \frac{g_m}{2\pi \cdot f_Z} \cdot \frac{Vr}{Vout}$$

where:

Equation 12

$$f_Z = \frac{1}{2\pi \cdot C_{out} \cdot R_{TOT}}$$

and:

Equation 13

$$R_{TOT} = ESR + R_{VESR}$$

Moreover, the C_{INT} capacitor must meet the following condition:

Equation 14

$$f_{SW} > k \cdot f_Z = \frac{k}{2\pi \cdot C_{out} \cdot R_{TOT}}$$

where R_{TOT} is the sum of the ESR of the output capacitor and the equivalent ESR given by the Virtual-ESR Network (R_{VESR}). The k parameter must be greater than unity (k > 3) and determines the minimum integrator capacitor value C_{INT}:

Equation 15

$$C_{INT} > \frac{g_m}{2\pi \cdot \left(\frac{f_{SW}}{k} - f_Z\right)} \cdot \frac{Vr}{Vout}$$

The capacitor of the Virtual-ESR Network, C, is chosen as follow

Equation 16

$$C > 5 \cdot C_{INT}$$

and R is calculated to provide the desired triangular ripple voltage:

Equation 17

$$R = \frac{L}{R_{VESR} \cdot C}$$

Finally the R1 resistor is calculated according to *Equation 18*:

Equation 18

$$R1 = \frac{R \cdot \left(\frac{1}{\pi \cdot f_Z \cdot C}\right)}{R - \frac{1}{\pi \cdot f_Z \cdot C}}$$

7.1.3 Pulse-skip and no-audible pulse-skip modes

High efficiency at light load conditions is achieved by PM6675S by entering the Pulse-Skip Mode (if enabled). At light load conditions the zero-crossing comparator truncates the low-side switch On-Time as soon as the inductor current becomes negative; in this way the comparator determines the On-Time duration instead of the output ripple.
(see *Figure 37*).

Figure 37. Inductor current and output voltage at light load with Pulse-Skip

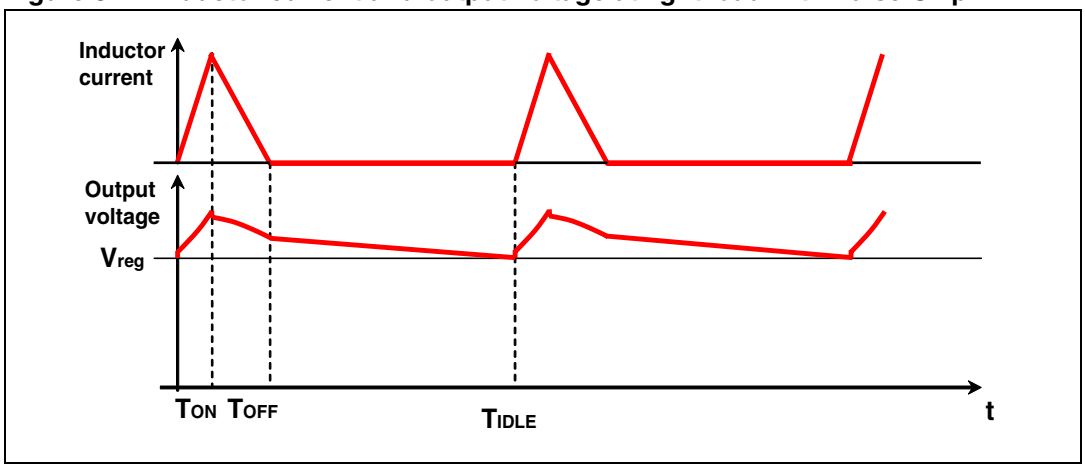

As a consequence, the output capacitor is left floating and its discharge depends solely on the current drained from the load. When the output ripple on the pin COMP falls under the reference, a new shot is triggered and the next cycle begins. The Pulse-Skip mode is naturally obtained enabling the zero-crossing comparator and automatically takes part in the COT algorithm when the inductor current is about half the ripple current amount, i.e. migrating from continuous conduction mode (C.C.M.) to discontinuous conduction mode (D.C.M.).

The output current threshold related to the transition between PWM Mode and Pulse-Skip Mode can be approximately calculated as:

Equation 19

$$I_{LOAD}(PWM2Skip) = \frac{V_{IN} - V_{OUT}}{2 \cdot L} \cdot T_{ON}$$

At higher loads, the inductor current never crosses the zero and the device works in pure PWM mode with a switching frequency around the nominal value.

A physiological consequence of Pulse-Skip Mode is a more noisy and asynchronous (than normal conditions) output, mainly due to very low load. If the Pulse-Skip is not compatible with the application, the PM6675S allows the user to choose between forced-PWM and No-Audible Pulse-Skip alternative modes (see *Section 7.1.4: Mode-of-operation selection on page 30* for details).

No-audible pulse-skip mode

Some audio-noise sensitive applications cannot accept the switching frequency to enter the audible range as it is possible in Pulse-Skip mode with very light loads. For this reason, the PM6675S implements an additional feature to maintain a minimum switching frequency of 33kHz despite a slight efficiency loss. At very light load conditions, if any switching cycle has taken place within 30µs (typ.) since the last one (because of the output voltage is still higher than the reference), a No-Audible Pulse-Skip cycle begins. The low-side MOSFET is turned on and the output is driven to fall until the reference point has been crossed. Then, the high-side switch is turned on for a T_{ON} period and, once it has expired, the synchronous rectifier is enabled until the inductor current reaches the zero-crossing threshold (see *Figure 38*).

Figure 38. Inductor current and output voltage at light load with non-audible pulse-skip

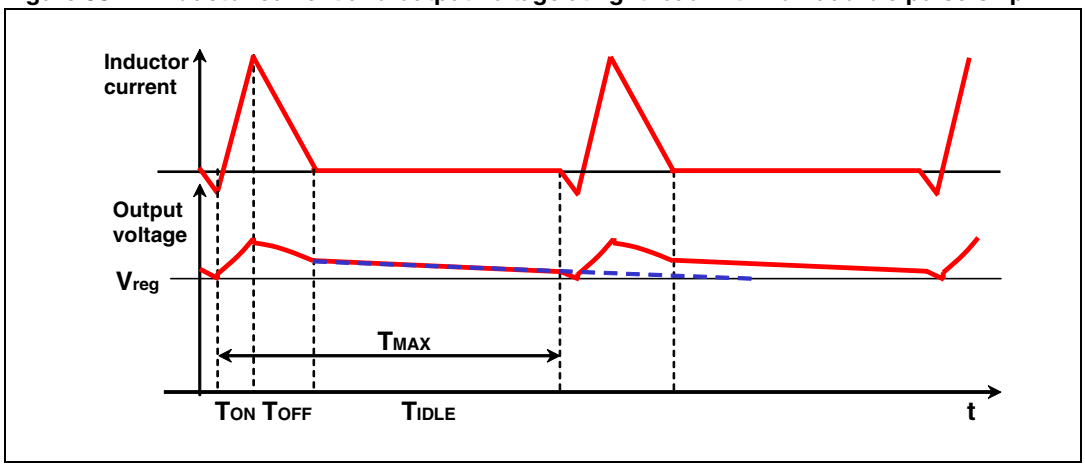

For frequencies higher than 33 kHz (due to heavier loads) the device works in the same way as in Pulse-Skip mode. It is important to notice that in both Pulse-Skip and No-Audible Pulse-Skip modes, the switching frequency changes not only with the load but also with the input voltage.

7.1.4 Mode-of-operation selection

Figure 39. VSEL and NOSKIP multifunction pin configurations

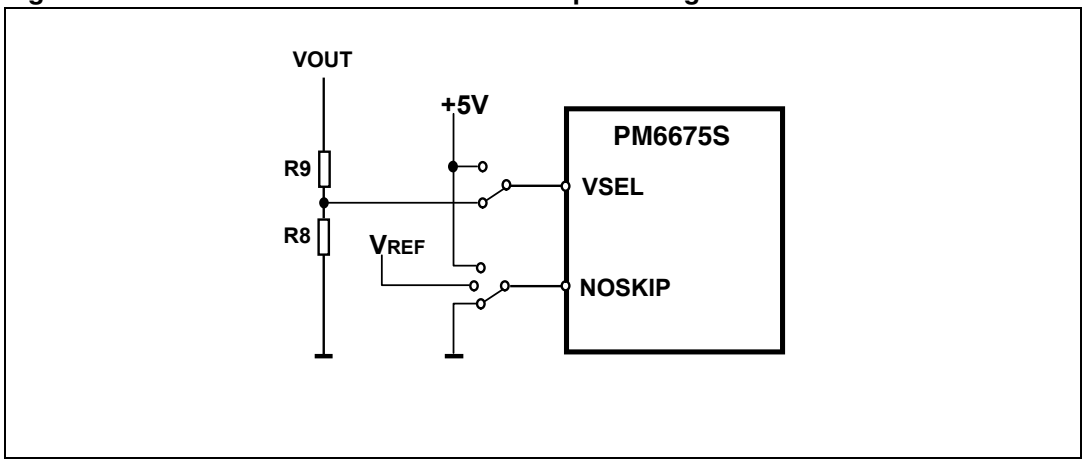

The PM6675S has been designed to satisfy the widest range of applications. The device is provided with some multilevel pins which allow the user to choose the appropriate configuration. The VSEL pin is used to firstly decide between fixed preset or adjustable (user defined) output voltages.

When the VSEL pin is connected to +5 V, the PM6675S sets the switching section output voltage to 1.5 V without the need of an external divider.

Applications requiring different output voltages can be managed by PM6675S simply setting the adjustable mode. Consider that if the VSEL pin voltage is higher than 4 V, the fixed output mode is selected. When connecting an external divider to the VSEL pin, it is used as negative input of the error amplifier and the output voltage is given by expression (20).

Equation 20

$$VOUT_{ADJ} = 0.6 \cdot \frac{R8 + R9}{R8}$$

The output voltage can be set in the range from 0.6 V to 3.3 V.

The NOSKIP is the power saving algorithm selector: if tied to +5 V, the forced-PWM (fixed frequency) control is performed. If grounded or connected to VREF pin (1.237 V reference voltage), the Pulse-Skip or Non-Audible Pulse-Skip Modes are respectively selected.

Table 8. Mode-of-operation settings summary

VSEL	NOSKIP	VOUT	Operating mode
V_{VSEL} > 4.3 V	V_{NOSKIP} > 4.2 V	1.5 V	Forced-PWM
	1V <V_{NOSKIP} < 3.5 V		Non-audible pulse-skip
	< 0.5 V		Pulse-skip
V_{VSEL} < 3.7 V	V_{NOSKIP} > 4.2 V	ADJ	Forced-PWM
	1V <V_{NOSKIP} < 3.5 V		Non-audible pulse-skip
	V_{NOSKIP} < 0.5 V		Pulse-skip

7.1.5 Current sensing and current limit

The PM6675S switching controller uses a valley current sensing algorithm to properly handle the current limit protection and the inductor current zero-crossing information. The current is detected during the conduction time of the low-side MOSFET. The current sensing element is the on-resistance of the low-side switch. The sensing scheme is visible in *Figure 40*.

Figure 40. Current sensing scheme

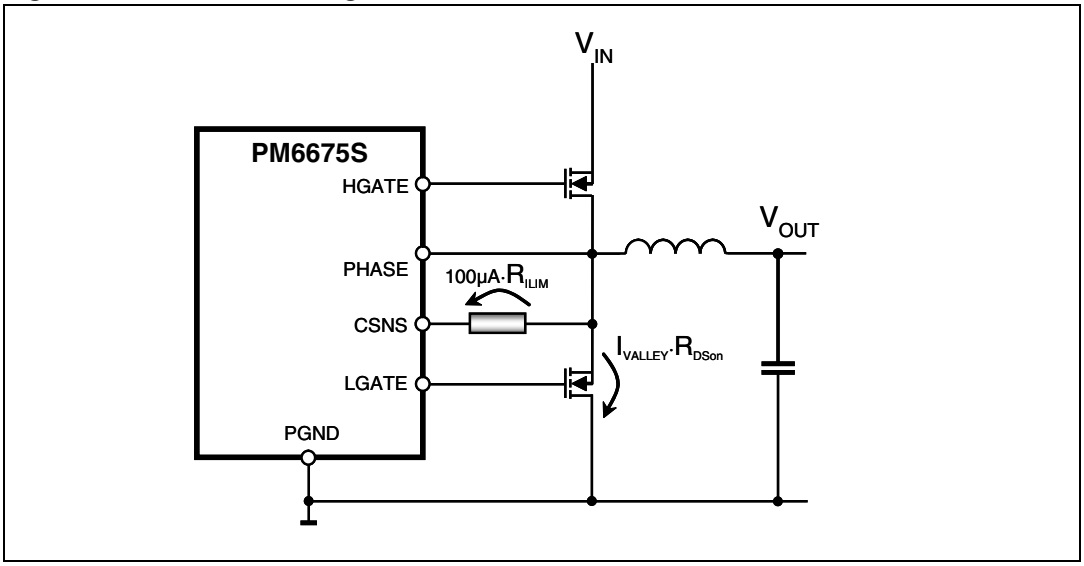

An internal 100 µA current source is connected to C_{SNS} pin that is also the non-inverting input of the positive current limit comparator. When the voltage drop developed across the sensing parameter equals the voltage drop across the programming resistor R_{ILIM}, the controller skips subsequent cycles until the overcurrent condition is detected or the output UV protection latches off the device (see *Section 7.1.11: Switching section OV and UV protections on page 34*).

Referring to *Figure 40*, the $R_{DS(on)}$ sensing technique allows high efficiency performance without the need for an external sensing resistor. The on-resistance of the MOSFET is affected by temperature drift and nominal value spread of the parameter itself; this must be considered during the R_{ILIM} setting resistor design.

It must be taken into account that the current limit circuit actually regulates the inductor valley current. This means that R_{ILIM} must be calculated to set a limit threshold given by the maximum DC output current plus half of the inductor ripple current:

Equation 21

$$I_{CL} = 100\mu A \cdot \frac{R_{ILIM}}{R_{DSon}}$$

The PM6675S provides also a fixed negative current limit to prevent excessive reverse inductor current when the switching section sinks current from the load in forced-PWM (3rd quadrant working conditions). This negative current limit threshold is measured between PHASE and PGND pins, comparing the drop magnitude on PHASE pin with an internal 110 mV fixed threshold.

7.1.6 POR, UVLO and soft-start

The PM6675S automatically performs an internal startup sequence during the rising phase of the analog supply of the device (AVCC). The switching controller remains in a stand-by state until AVCC crosses the upper UVLO threshold (4.25 V typ.), keeping active the internal discharge MOSFETs (only if AVCC > 1V).

The soft-start allows a gradual increase of the internal current limit threshold during startup reducing the input/output surge currents. At the beginning of start-up, the PM6675S current limit is set to 25 % of nominal value and the Under Voltage Protection is disabled. Then, the current limit threshold is sequentially brought to 100 % in four steps of approximately 750 µs (*Figure 41*).

Figure 41. Soft-start waveforms

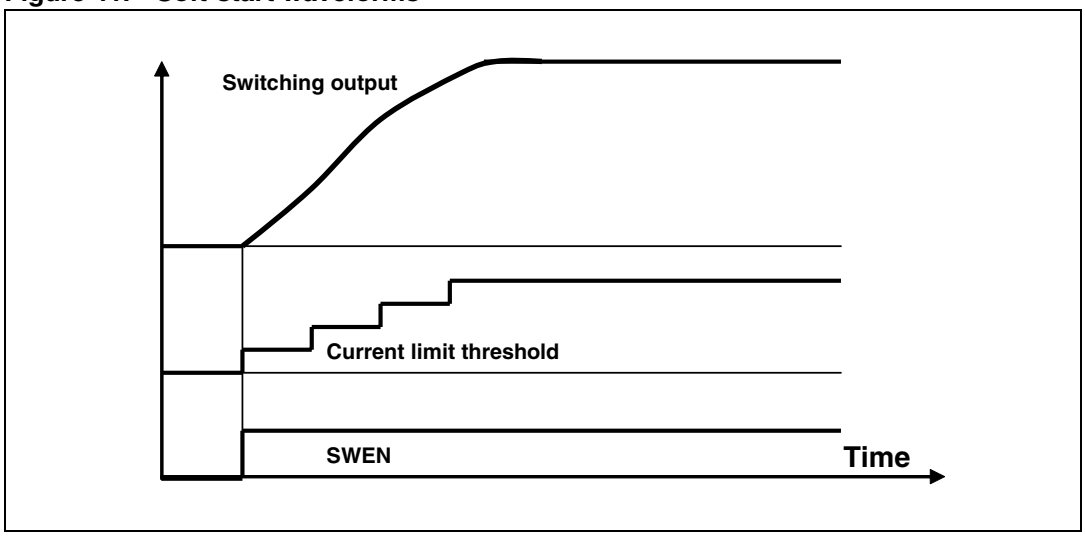

After a fixed 3ms total time, the soft-start finishes and UVP is released: if the output voltage doesn't reach the under voltage threshold within soft-start duration, the UVP condition is detected and the device performs a soft-end and latches off. Depending on the load conditions, the inductor current may or may not reach the nominal value of the current limit during the soft-start (*Figure 42* shows two examples).

Figure 42. Soft-start at heavy load (a) and short-circuit (b) conditions, Pulse-Skip enabled

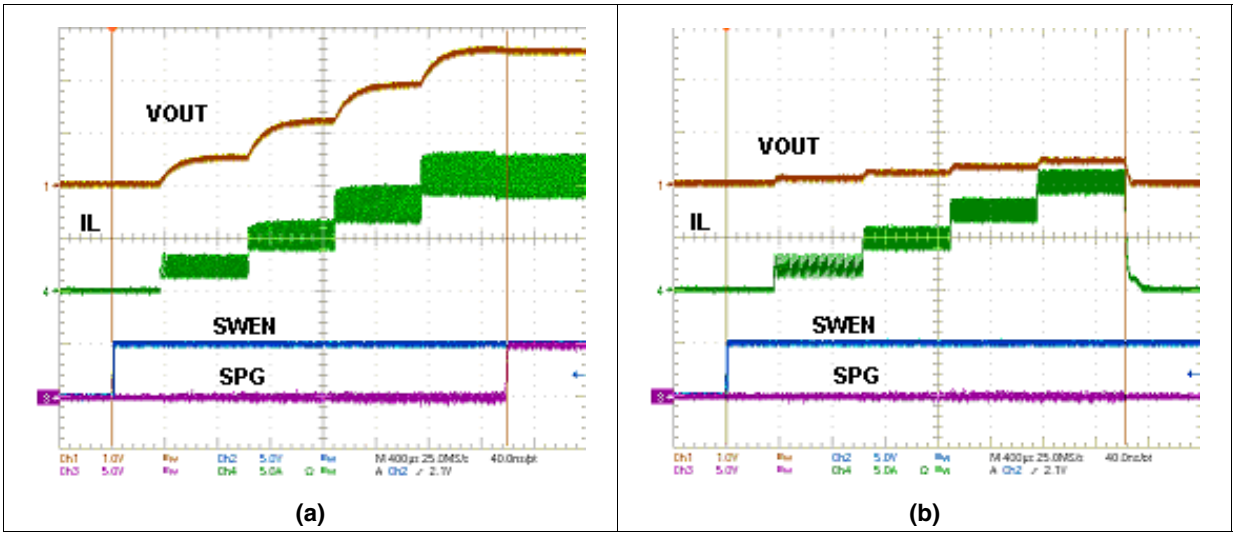

7.1.7 Switching section power good signal

The SPG pin is an open drain output used to monitor output voltage through VSNS (in fixed output voltage mode) or VSEL (in adjustable output voltage mode) pins and is enabled after the soft-start timer has expired. The SPG signal is held low if the output voltage drops 10% below or rises 10 % above the nominal regulated value. The SPG output can sink current up to 4 mA.

7.1.8 Switching section output discharge

Active soft-end of the output occurs when the SWEN (SWitching ENable) is forced low. When the switching section is turned off, an internal 25 Ω resistor discharges the output through the VSNS pin.

Figure 43. Switching section soft-end

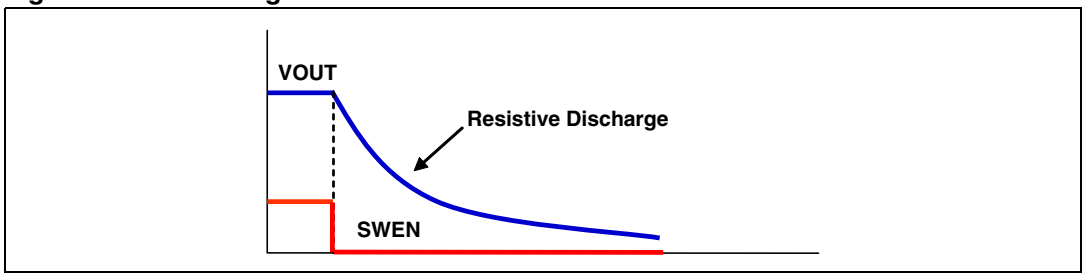

7.1.9 Gate drivers

The integrated high-current gate drivers allow using different power MOSFETs. The high-side driver uses a bootstrap circuit which is supplied by the +5 V rail. The BOOT and PHASE pins work respectively as supply and return path for the high-side driver, while the low-side driver is directly fed through VCC and PGND pins.

An important feature of the PM6675S gate drivers is the Adaptive Anti-Cross-Conduction circuitry, which prevents high-side and low-side MOSFETs from being turned on at the same time. When the high-side MOSFET is turned off, the voltage at the PHASE node begins to fall. The low-side MOSFET is turned on only when the voltage at the PHASE node reaches an internal threshold (2.5 V typ.). Similarly, when the low-side MOSFET is turned off, the high-side one remains off until the LGATE pin voltage is above 1 V.

The power dissipation of the drivers is a function of the total gate charge of the external power MOSFETs and the switching frequency, as shown in the following equation:

Equation 22

$$P_D(\text{driver}) = V_{DRV} \cdot Q_g \cdot f_{SW}$$

The low-side driver has been designed to have a low-resistance pull-down transistor (0.6 Ω typ.) in order to prevent undesired start-up of the low-side MOSFET due to the Miller effect.

7.1.10 Reference voltage and bandgap

The 1.237 V internal bandgap reference has a granted accuracy of ±1 % over the 0 °C to 85 °C temperature range. The VREF pin is a buffered replica of the bandgap voltage. It can supply up to ±100 µA and is suitable to set the intermediate level of NOSKIP multifunction pin. A 100 nF (min.) bypass capacitor toward SGND is required to enhance noise rejection. If VREF falls below 0.8 V (typ.), the system detects a fault condition and all the circuitry is turned off.

An internal divider derives a 0.6 V ± 1 % voltage (Vr) from the bandgap. This voltage is used as reference for both the switching and the linear sections. The Over-Voltage Protection, the Under-Voltage Protection and the power-good signals are also referred to Vr.

7.1.11 Switching section OV and UV protections

When the switching output voltage is about 115 % of its nominal value, a latched Over-Voltage Protection (OVP) occurs. In this case the synchronous rectifier immediately turns on while the high-side MOSFET turns off. The output capacitor is rapidly discharged and the load is preserved from being damaged. The OVP is also active during the soft-start. Once an OVP has taken part, a toggle on SWEN pin or a Power-On-Reset is necessary to exit from the latched state.

When the switching output voltage is below 70 % of its nominal value, a latched Under-Voltage Protection occurs. This event causes the switching section to be immediately disabled and both switches to be opened. The controller performs a soft-end and the output is eventually kept to ground, turning the low side MOSFET on when the voltage is lower than 400 mV.

The Under-Voltage Protection circuit is enabled only at the end of the soft-start. Once an UVP has taken part, a toggle on SWEN pin or a Power-On-Reset is necessary to clear the fault state and restart the section.

7.1.12 Device thermal protection

The internal control circuitry of the PM6675S self-monitors the junction temperature and turns all outputs off when the 150 °C limit has been overrun. This event causes the switching section to be immediately disabled and both switches to be opened. The controller performs a soft-end and both the outputs are eventually kept to ground, then the low side MOSFET is turned on when the voltage of the switching section is lower than 400 mV.

The thermal fault is a latched protection and, in normal operating conditions it is restored by a Power-On Reset or toggling SWEN and LEN pins at the same time.

Table 9. Switching section OV, UV and OT Faults management

Fault	Conditions	Action
Over voltage	VOUT > 115 % of the nominal value	LGATE pin is forced high and the device latches off. Exit by a Power-On Reset or toggling SWEN
Under voltage	VOUT < 70 % of the nominal value	LGATE pin is forced high after the soft-end, then the device latches off. Exit by a Power-On Reset or toggling SWEN.
Junction over temperature	T_J > +150 °C	LGATE pin is forced high after the soft-end, then the device latches off. Exit by a Power-On Reset or toggling SWEN and LEN after 15°C temperature drop.

7.2 LDO linear regulator section

The independent Low-Drop-Out (LDO) linear regulator has been designed to sink and source up to 2 A peak current and 1 A continuously. The LDO output voltage can be adjusted in the range 0.6 V to 3.3 V simply connecting a resistor divider as shown in *Figure 44*.

Equation 23

$$VLDO_{ADJ} = 0.6 \cdot \frac{R19 + R20}{R20}$$

Figure 44. LDO output voltage selection

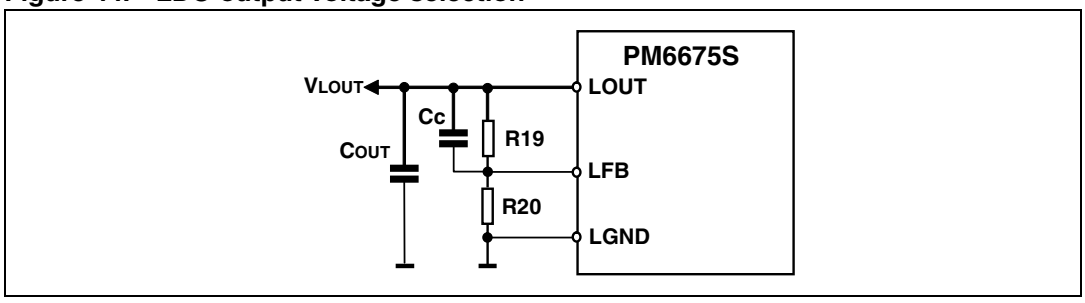

A compensation capacitor Cc must be added to adjust the dynamic response of the loop. The value of Cc is calculated according to the desired bandwidth of the LDO regulator and depends on the value of the feedback resistors. In most of applications the pole due to the compensation capacitor is placed at 100-200 kHz (equation 24).

Equation 24

$$f_p = \frac{1}{2\pi(R19 \oplus R20) \cdot C_C} = 200kHz$$

The LIN input can be connected to the switching section output for compact solutions or to a lower supply, if available in the system, in order to reduce the power dissipation of the LDO.

A minimum output capacitance of 20 µF (2x10 µF MLCC capacitors) is enough to assure stability and fast load transient response.

7.2.1 LDO section current limit

The LDO regulator can handle up to ±2 Apk, depending on the LDO input voltage and the LILIM pin setting. The output current is limited to ±1 A or ±2 A if the LILIM pin is connected to SGND or AVCC respectively (*Figure 45*).

Figure 45. LDO current limit setting

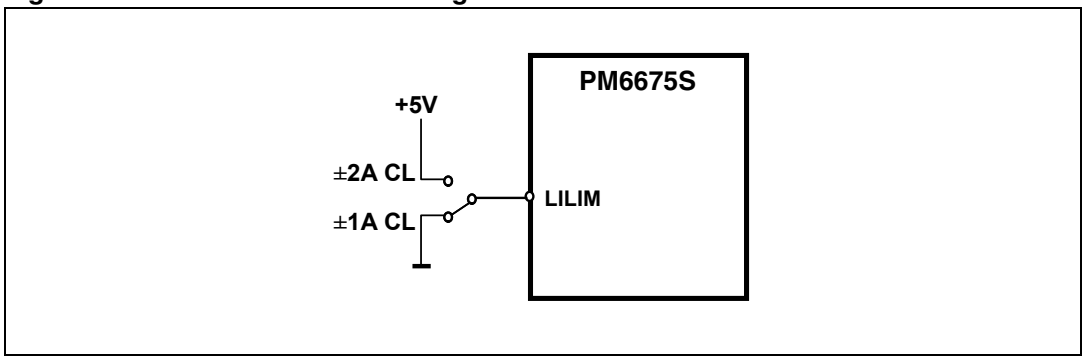

The maximum current that the LDO can source depends also on the input and output voltages. Due to the high side MOSFET of the output stage, the LDO cannot source the limit current at high output voltages. In *Figure 46* it is shown the maximum current that the LDO can source as function of the input and output voltages. For output voltages higher than 2 V, the maximum output current is limited as reported.

Figure 46. Maximum LDO source able output current vs input voltage

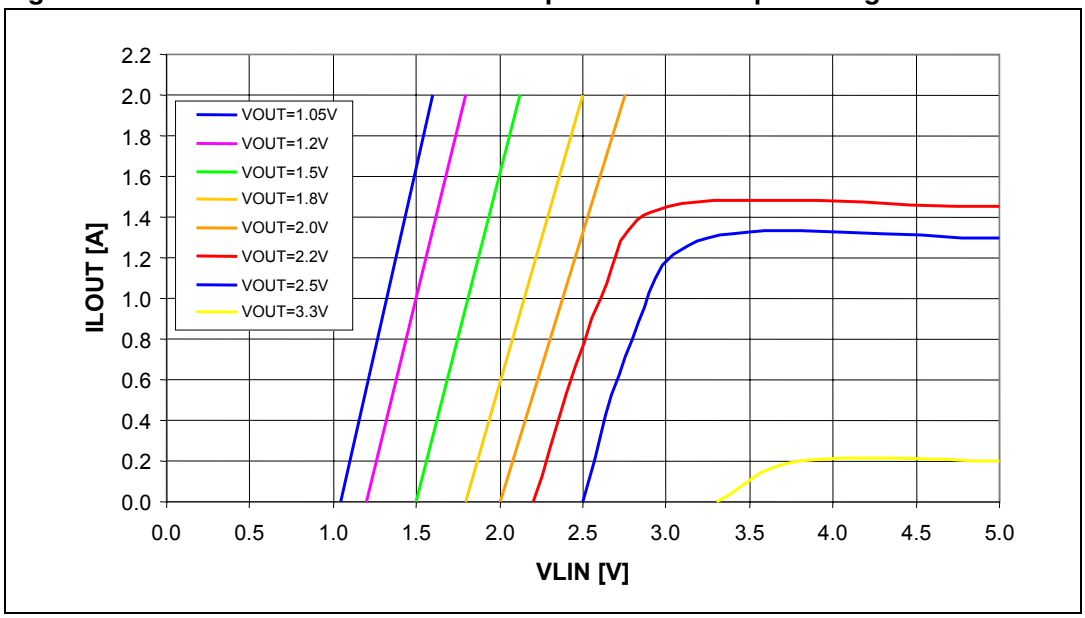

7.2.2 LDO section soft-start

The LDO section soft-start is performed by clamping the current limit. During startup, the LDO current limit voltage is set to 1A and the output voltage increases linearly. When the output voltage rises above 90 % of the nominal value, the current limit is released to 2 A according to the LILIM pin setting. At the end of the ramp-up phase of the soft-start, the LPG signal is masked for about 100 µs in order to ignore dynamic overshoot on the feedback pin.

7.2.3 LDO section power good signal

The LPG pin is an open drain output used to monitor the LDO output voltage through LFB pin.

The LPG signal is held low if the output voltage drops 10 % below or rises 10 % above the nominal regulated value. The LPG output can sink current up to 4 mA.

7.2.4 LDO section output discharge

Active soft-end of the LDO output occurs when the LEN (Linear ENable) is forced low. When the LDO section is turned off, an internal 25 Ω resistor, directly connected to the LOUT pin, discharges the output.

Figure 47. LDO section soft-end

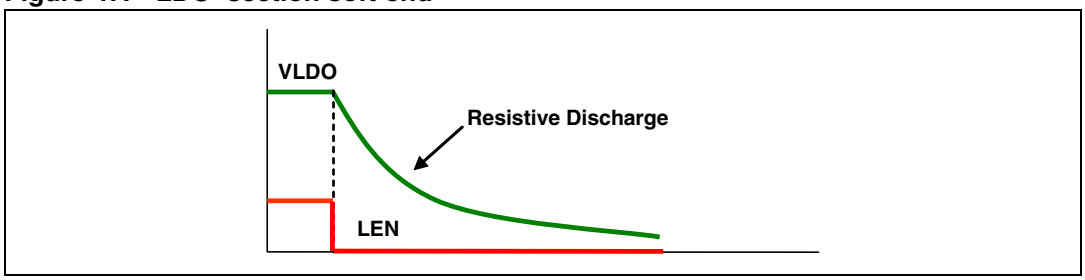

8 Application information

The purpose of this chapter is showing the design procedure of the switching section.

The design starts from three main specifications:

- The input voltage range, provided by the battery or the external supply. The two extreme values (V_{INMAX} and V_{INmin}) are important for the design.
- The maximum load current, indicated with $I_{LOAD,MAX}$.
- The maximum allowed output voltage ripple $V_{RIPPLE,MAX}$.

It's also possible that specific designs should involve other specifications.

The following paragraphs will guide the user into a step-by-step design.

8.1 External components selection

The PM6675S uses a pseudo-fixed frequency, Constant On-Time (COT) controller as the core of the switching section. The switching frequency can be set by connecting an external divider to the VOSC pin. The voltage seen at this pin must be greater than 0.8V and lower than 2 V in order to ensure system linearity.

Nearly constant switching frequency is achieved by the system loop in steady-state operating conditions by varying the On-Time duration, avoiding thus the need for a clock generator. The On-Time one shot duration is directly proportional to the output voltage, sensed at VSNS pin, and inversely proportional to the input voltage, sensed at the VOSC pin, as follows:

Equation 25

$$T_{ON} = K_{OSC}\frac{V_{SNS}}{V_{OSC}} + \tau$$

where K_{OSC} is a constant value (130 ns typ.) and τ is the internal propagation delay (40 ns typ.).

The duty cycle of the buck converter is, in under steady state conditions, given by

Equation 26

$$D = \frac{V_{OUT}}{V_{IN}}$$

The switching frequency is thus calculated as

Equation 27

$$f_{SW} = \frac{D}{T_{ON}} = \frac{\frac{V_{OUT}}{V_{IN}}}{K_{OSC}\cdot\frac{V_{SNS}}{V_{OSC}}} = \frac{\alpha_{OSC}}{\alpha_{OUT}}\cdot\frac{1}{K_{OSC}}$$

where

Equation 28a

$$\alpha_{OSC} = \frac{V_{OSC}}{V_{IN}}$$

Equation 28b

$$\alpha_{OUT} = \frac{V_{SNS}}{V_{OUT}}$$

Referring to the typical application schematic (figure in cover page and *Figure 33*), the final expression is then:

Equation 29

$$f_{SW} = \frac{\alpha_{OSC}}{K_{OSC}} = \frac{R_2}{R_1 + R_2} \cdot \frac{1}{K_{OSC}}$$

The switching frequency directly affects two parameters:

- Inductor size: greater frequencies mean smaller inductances. In notebook applications, real estate solutions (i.e. low-profile power inductors) are mandatory also with high saturation and r.m.s. currents.
- Efficiency: switching losses are proportional to the frequency. Generally, higher frequencies imply lower efficiency.

Even if the switching frequency is theoretically independent from battery and output voltages, parasitic parameters involved in power path (like MOSFETs on-resistance and inductor DCR) introduce voltage drops responsible for a slight dependence on load current.

In addition, the internal delay is cause of a light dependence from input voltage.

Table 10. Typical values for switching frequency selection

R1 (kΩ)	R2 (kΩ)	Approx switching frequency (kHz)
330	11	250
330	13	300
330	15	350
330	18	400
330	20	450
330	22	500

8.1.1 Inductor selection

Once the switching frequency has been defined, the inductance value depends on the desired inductor ripple current. Low inductance value means great ripple current that brings poor efficiency and great output noise. On the other hand a great current ripple is desirable for fast transient response when a load step is applied.

High inductance brings to good efficiency but the transient response is critical, especially if V_{INmin} - V_{OUT} is little. Moreover a minimum output ripple voltage is necessary to assure system stability and jitter-free operations (see *Section 8.1.3: Output capacitor selection on page 42*). The product of the output capacitor ESR multiplied by the inductor ripple current must be taken in consideration. A good trade-off between the transient response time, the efficiency, the cost and the size is choosing the inductance value in order to maintain the inductor ripple current between 20 % and 50 % (usually 40 %) of the maximum output current.

The maximum inductor ripple current, $\Delta I_{L,MAX}$, occurs at the maximum input voltage.

Given these considerations, the inductance value can be calculated using the following expression:

Equation 30

$$L = \frac{V_{IN} - V_{OUT}}{fsw \cdot \Delta I_L} \cdot \frac{V_{OUT}}{V_{IN}}$$

where f_{SW} is the switching frequency, V_{IN} is the input voltage, V_{OUT} is the output voltage and ΔI_L is the inductor ripple current.

Once the inductor value is determined, the inductor ripple current is then recalculated:

Equation 31

$$\Delta I_{L,MAX} = \frac{V_{IN,MAX} - V_{OUT}}{fsw \cdot L} \cdot \frac{V_{OUT}}{V_{IN,MAX}}$$

The next step is the calculation of the maximum r.m.s. inductor current:

Equation 32

$$I_{L,RMS} = \sqrt{(I_{LOAD,MAX})^2 + \frac{(\Delta I_{L,MAX})^2}{12}}$$

The inductor must have an r.m.s. current greater than $I_{L,RMS}$ in order to assure thermal stability.

Then the calculation of the maximum inductor peak current follows:

Equation 33

$$I_{L,PEAK} = I_{LOAD,MAX} + \frac{\Delta I_{L,MAX}}{2}$$

$I_{L,PEAK}$ is important when choosing the inductor, in term of its saturation current.

The saturation current of the inductor should be greater than $I_{L,PEAK}$ as well as for case of hard saturation core inductors. Using soft-ferrite cores is possible (but not advisable) to push the inductor working near its saturation current.

In *Table 11* some inductors suitable for notebook applications are listed.

Table 11. Evaluated inductors (@fsw = 400 kHz)

Manufacturer	Series	Inductance (µH)	+40 °C RMS current (A)	-30 % saturation current (A)
COILCRAFT	MLC1538-102	1	13.4	21.0
COILCRAFT	MLC1240-901	0.9	12.4	24.5
COILCRAFT	MVR1261C-112	1.1	20	20
WURTH	7443552100	1	16	20
COILTRONICS	HC8-1R2	1.2	16.0	25.4

In Pulse-Skip Mode, low inductance values produce a better efficiency versus load curve, while higher values result in higher full-load efficiency because of the smaller current ripple.

8.1.2 Input capacitor selection

In a buck topology converter the current that flows through the input capacitor is pulsed and with zero average value. The RMS input current can be calculated as follows:

Equation 34

$$I_{CinRMS} = \sqrt{I_{LOAD}^{2} \cdot D \cdot (1-D) + \frac{1}{12} D \cdot (\Delta I_L)^2}$$

Neglecting the second term, the equation 10 is reduced to:

Equation 35

$$I_{CinRMS} = I_{LOAD} \sqrt{D \cdot (1-D)}$$

The losses due to the input capacitor are thus maximized when the duty-cycle is 0.5:

Equation 36

$$P_{loss} = ESR_{Cin} \cdot I_{CinRMS}(max)^2 = ESR_{Cin} \cdot (0.5 \cdot I_{LOAD}(max))^2$$

The input capacitor should be selected with a RMS rated current higher than I_{CINRMS}(max). Tantalum capacitors are good in terms of low ESR and small size, but they occasionally can burn out if subjected to very high current during operation. Multi-Layers-Ceramic-Capacitors (MLCC) have usually a higher RMS current rating with smaller size and they remain the best choice. The drawback is their quite high cost.

It must be taken into account that in some MLCC the capacitance decreases when the operating voltage is near the rated voltage. In *Table 12* some MLCC suitable for most of applications are listed.

Table 12. Evaluated MLCC for input filtering

Manufacturer	Series	Capacitance (µF)	Rated voltage (V)	Maximum Irms @100 kHz (A)
TAIYO YUDEN	UMK325BJ106KM-T	10	50	2
TAIYO YUDEN	GMK316F106ZL-T	10	35	2.2
TAIYO YUDEN	GMK325F106ZH-T	10	35	2.2
TAIYO YUDEN	GMK325BJ106KN	10	35	2.5
TDK	C3225X5R1E106M	10	25	

8.1.3 Output capacitor selection

Using tantalum or electrolytic capacitors, the selection is made referring to ESR and voltage rating rather than by a specific capacitance value.

The output capacitor has to satisfy the output voltage ripple requirements. At a given switching frequency, small inductor values are useful to reduce the size of the choke but increase the inductor current ripple. Thus, to reduce the output voltage ripple a low ESR capacitor is required.

To reduce jitter noise between different switching regulators in the system, it is preferable to work with an output voltage ripple greater than 25 mV.

Concerning the load transient requirements, the Equivalent Series Resistance (ESR) of the output capacitor must satisfy the following relationship:

Equation 37

$$ESR \leq \frac{V_{RIPPLE,MAX}}{\Delta I_{L,MAX}}$$

where V_{RIPPLE} is the maximum tolerable ripple voltage.

In addition, the ESR must be high enough to meet stability requirements. The output capacitor zero must be lower than the switching frequency:

Equation 38

$$f_{SW} > f_Z = \frac{1}{2\pi \cdot ESR \cdot C_{out}}$$

If ceramic capacitors are used, the output voltage ripple due to inductor current ripple is negligible. Then the inductance should be smaller, reducing the size of the choke. In this case it is important that output capacitor can adsorb the inductor energy without generating an over-voltage condition when the system changes from a full load to a no load condition.

The minimum output capacitance can be chosen by the following equation:

Equation 39

$$C_{OUT,min} = \frac{L \cdot I_{LOAD,MAX}^2}{Vf^2 - Vi^2}$$

where Vf is the output capacitor voltage after the load transient, while Vi is the output capacitor voltage before the load transient.

In *Table 13* are listed some tested polymer capacitors.

Table 13. Evaluated output capacitors

Manufacturer	Series	Capacitance (µF)	Rated voltage (V)	ESR max @100 kHz (mΩ)
SANYO	4TPE220MF	220	4 V	15 to 25
	4TPE150MI	220	4 V	18
	4TPC220M	220	4 V	40
HITACHI	TNCB OE227MTRYF	220	2.5 V	25

8.1.4 MOSFETs selection

In a notebook application, power management efficiency is a high level requirement. The power dissipation on the power switches becomes an important factor in the selection of switches. Losses of high-side and low-side MOSFETs depend on their working condition.

Considering the high-side MOSFET, the power dissipation is calculated as:

Equation 40

$$P_{DHighSide} = P_{conduction} + P_{switching}$$

Maximum conduction losses are approximately given by:

Equation 41

$$P_{conduction} = R_{DSon} \cdot \frac{V_{OUT}}{V_{IN.min}} \cdot I_{LOAD,MAX}^2$$

where $R_{DS(on)}$ is the drain-source on-resistance of the control MOSFET.

Switching losses are approximately given by:

Equation 42

$$P_{switching} = \frac{V_{IN} \cdot (I_{LOAD}(max) - \frac{\Delta I_L}{2}) \cdot t_{on} \cdot f_{sw}}{2} + \frac{V_{IN} \cdot (I_{LOAD}(max) + \frac{\Delta I_L}{2}) \cdot t_{off} \cdot f_{sw}}{2}$$

where t_{ON} and t_{OFF} are the turn-on and turn-off times of the MOSFET and depend on the gate-driver current capability and the gate charge Q_{gate}. A greater efficiency is achieved with low R_{DSon}. Unfortunately low R_{DSon} MOSFETs have a great gate charge.

As general rule, the $R_{DS(on)}$ x Q_{gate} product should be minimized to find the suitable MOSFET.

Logic-level MOSFETs are recommended, as long as low-side and high-side gate drivers are powered by V_{VCC} = +5 V. The breakdown voltage of the MOSFETs (V_{BRDSS}) must be greater than the maximum input voltage V_{INmax}.

Below some tested high-side MOSFETs are listed.

Table 14. Evaluated high-side MOSFETs

Manufacturer	Type	$R_{DS(on)}$ (mΩ)	Gate charge (nC)	Rated reverse voltage (V)
ST	STS12NH3LL	10.5	12	30
IR	IRF7811	9	18	30

In buck converters the power dissipation of the synchronous MOSFET is mainly due to conduction losses:

Equation 43

$$P_{DLowSide} \cong P_{conduction}$$

Maximum conduction losses occur at the maximum input voltage:

Equation 44

$$P_{conduction} = R_{DSon} \cdot \left(1 - \frac{V_{OUT}}{V_{IN,MAX}}\right) \cdot I_{LOAD,MAX}^{2}$$

The synchronous rectifier should have the lowest $R_{DS(on)}$ as possible. When the high-side MOSFET turns on, high d_V/d_t of the phase node can bring up even the low-side gate through its gate-drain capacitance C_{RRS}, causing a cross-conduction problem. Once again, the choice of the low-side MOSFET is a trade-off between on resistance and gate charge; a good selection should minimizes the ratio C_{RSS} / C_{GS} where

Equation 45

$$C_{GS} = C_{ISS} - C_{RSS}$$

Below some tested low-side MOSFETs are listed.

Table 15. Evaluated low-side MOSFETs

Manufacturer	Type	$R_{DS(on)}$ (mΩ)	$C_{GD} \setminus C_{GS}$	Rated reverse voltage (V)
ST	STS12NH3LL	13.5	0.069	30
ST	STS25NH3LL	4.0	0.011	30
IR	IRF7811	24	0.054	30

Dual N-MOS can be used in applications with lower output current.

Table 16 shows some suitable dual MOSFETs for applications requiring about 3 A.

Table 16. Suitable dual MOSFETs

Manufacturer	Type	R_{DSon} (mΩ)	Gate charge (nC)	Rated reverse voltage (V)
ST	STS8DNH3LL	25	10	30
IR	IRF7313	46	33	30

8.1.5 Diode selection

A rectifier across the synchronous switch is recommended. The rectifier works as a voltage clamp across the synchronous rectifier and reduces the negative inductor swing during the dead time between turning the high-side MOSFET off and the synchronous rectifier on. Moreover it increases the efficiency of the system.

Choose a schottky diode as long as its forward voltage drop is very little (0.3 V). The reverse voltage should be greater than the maximum input voltage V_{INmax} and a minimum recovery reverse charge is preferable. *Table 17* shows some evaluated diodes.

Table 17. Evaluated recirculation rectifiers

Manufacturer	Type	Forward voltage (V)	Rated reverse voltage (V)	Reverse current (μA)
ST	STPS1L30M	0.34	30	0.00039
ST	STPS1L30A	0.34	30	0.00039

8.1.6 VOUT current limit setting

The valley current limit is set by R_{CSNS} and must be chosen to support the maximum load current. The valley of the inductor current $I_{Lvalley}$ is:

Equation 46

$$I_{Lvalley} = I_{LOAD}(max) - \frac{\Delta I_L}{2}$$

The output current limit depends on the current ripple as shown in *Figure 48*:

Figure 48. Valley current limit waveforms

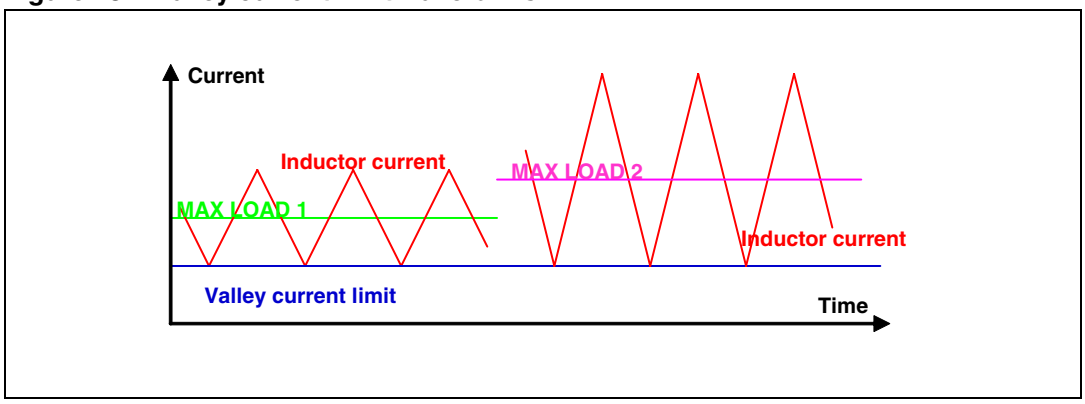

As the valley threshold is fixed, the greater the current ripple, the greater the DC output current will be. If an output current limit greater than $I_{LOAD}(max)$ over all the input voltage range is required, the minimum current ripple must be considered in the previous formula.

Then the resistor R_{CSNS} is:

Equation 47

$$R_{CSNS} = \frac{R_{DSon} \cdot I_{Lvalley}}{100uA}$$

where R_{DSon} is the drain-source on-resistance of the low-side switch. Consider the temperature effect and the worst case value in R_{DSon} calculation (typically +0.4 % / °C).

The accuracy of the valley current also depends on the offset of the internal comparator (±5 mV).

The negative valley-current limit (if the device works in forced-PWM mode) is given by:

Equation 48

$$I_{NEG} = \frac{110mV}{R_{DSon}}$$

8.1.7 All ceramic capacitors application

Design of external feedback network depends on the output voltage ripple across the output capacitors ESR. If the ripple is great enough (at least 20 mV), the compensation network simply consists of a C_{INT} capacitor.

Figure 49. Integrative compensation

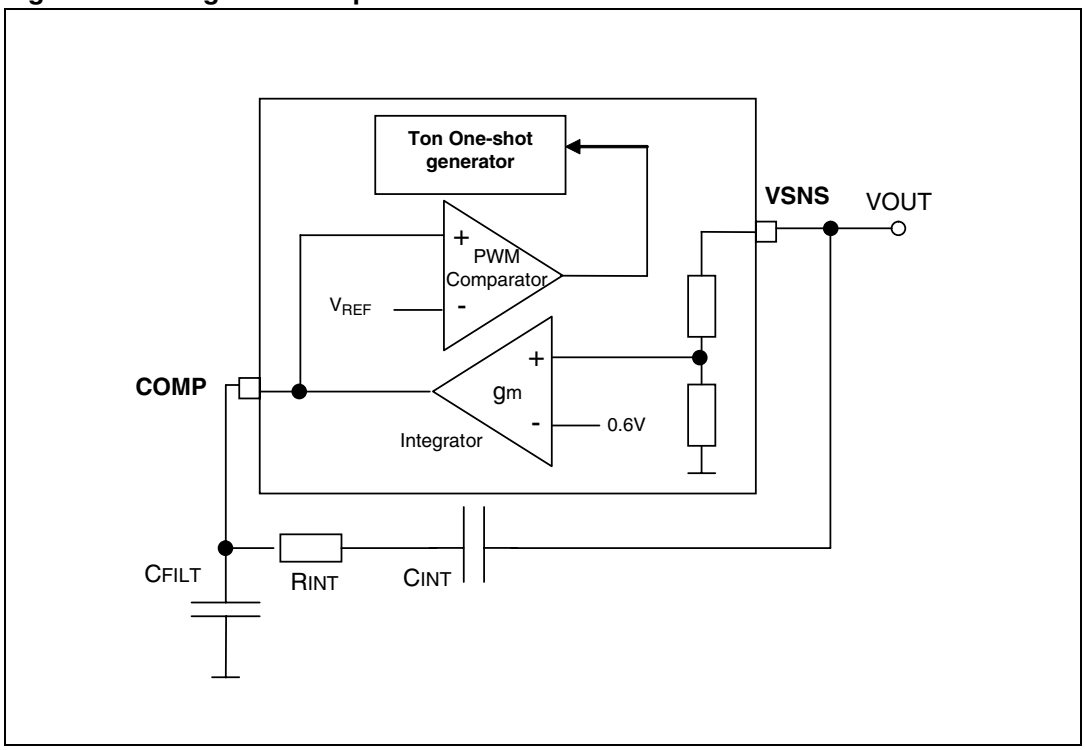

The stability of the system firstly depends on the output capacitor zero frequency. It must be verified that:

Equation 49

$$f_{SW} > k \cdot f_{Zout} = \frac{k}{2\pi \cdot R_{out} C_{out}}$$

where k is a free design parameter greater than unity (k > 3) . It determines the minimum integrator capacitor value C_{INT}:

Equation 50

$$C_{INT} > \frac{g_m}{2\pi \cdot \left(\frac{f_{SW}}{k} - f_{Zout} \right)} \cdot \frac{Vref}{Vo}$$

If the ripple on the COMP pin is greater than the integrator output dynamic (150 mV), an additional capacitor C_{filt} could be added in order to reduce its amplitude. If q is the desired attenuation factor of the output ripple, select:

Equation 51

$$C_{filt} = \frac{C_{INT} \cdot (1-q)}{q}$$

In order to reduce noise on the COMP pin, it's possible to introduce a resistor R_{INT} that, together with C_{INT} and C_{filt}, becomes a low pass filter. The cutoff frequency f_{CUT} must be much greater (10 or more times) than the switching frequency:

Equation 52

$$R_{INT} = \frac{1}{2\pi \cdot f_{CUT} \frac{C_{INT} \cdot C_{FILT}}{C_{INT} + C_{FILT}}}$$

For most applications both R_{INT} and C_{filt} are unnecessary.

If the ripple is very small (e.g. such as with ceramic capacitors), a further compensation network, called "Virtual ESR" network, is needed. This additional part generates a triangular ripple that substitutes the ESR output voltage ripple. The complete compensation scheme is represented in *Figure 50*.

Figure 50. Virtual ESR network

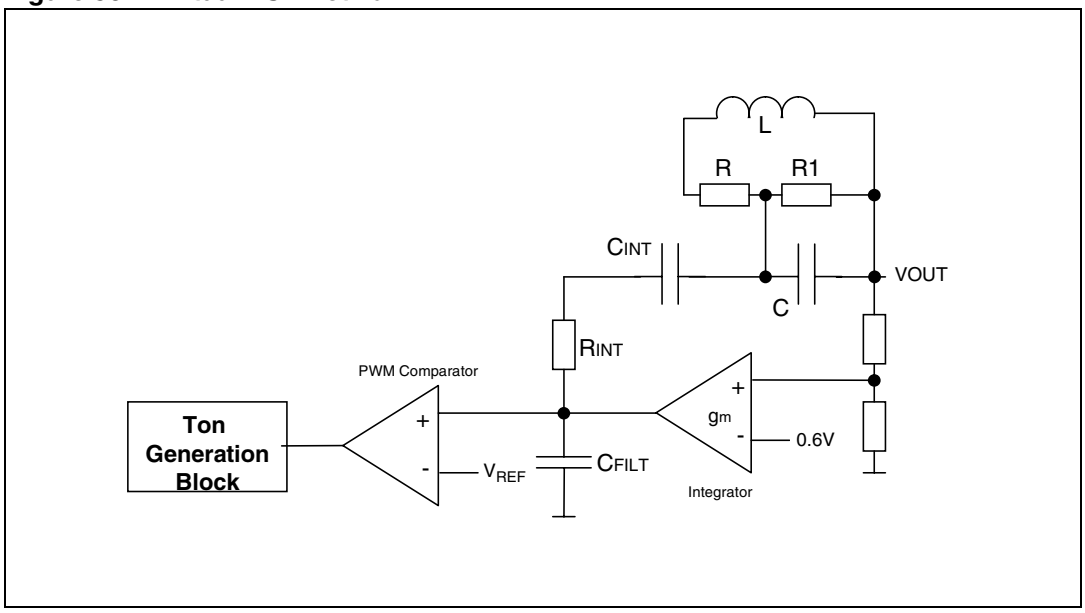

Select C as shown:

Equation 53

$$C > 5 \cdot C_{INT}$$

Then calculate R in order to have enough ripple voltage on the integrator input:

Equation 54

$$R = \frac{L}{R_{VESR} \cdot C}$$

Where R_{VESR} is the new virtual output capacitor ESR. A good trade-off is to consider an equivalent ESR of 30-50 mΩ , even though the choice depends on inductor current ripple.

Then choose R1 as follows:

Equation 55

$$R1 = \frac{R \cdot \left(\frac{1}{\pi \cdot f_Z \cdot C} \right)}{R - \frac{1}{\pi \cdot f_Z \cdot C}}$$

9 Package mechanical data

In order to meet environmental requirements, ST offers these devices in ECOPACK® packages. These packages have a Lead-free second level interconnect. The category of second Level Interconnect is marked on the package and on the inner box label, in compliance with JEDEC Standard JESD97. The maximum ratings related to soldering conditions are also marked on the inner box label. ECOPACK is an ST trademark. ECOPACK specifications are available at: www.st.com.

Table 18. VFQFPN-24 4 mm x 4 mm mechanical data

Dim.	mm.		
	Min	Typ	Max
A	0.80	0.90	1.00
A1		0.0	0.05
A2		0.65	0.80
D		4.00	
D1		3.75	
E		4.00	
E1		3.75	
θ			12°
P	0.24	0.42	0.60
e		0.50	
N		24.00	
Nd		6.00	
Ne		6.00	
L	0.30	0.40	0.50
b	0.18		0.30
D2	1.95	2.10	2.25
E2	1.95	2.10	2.25

Figure 51. Package dimensions

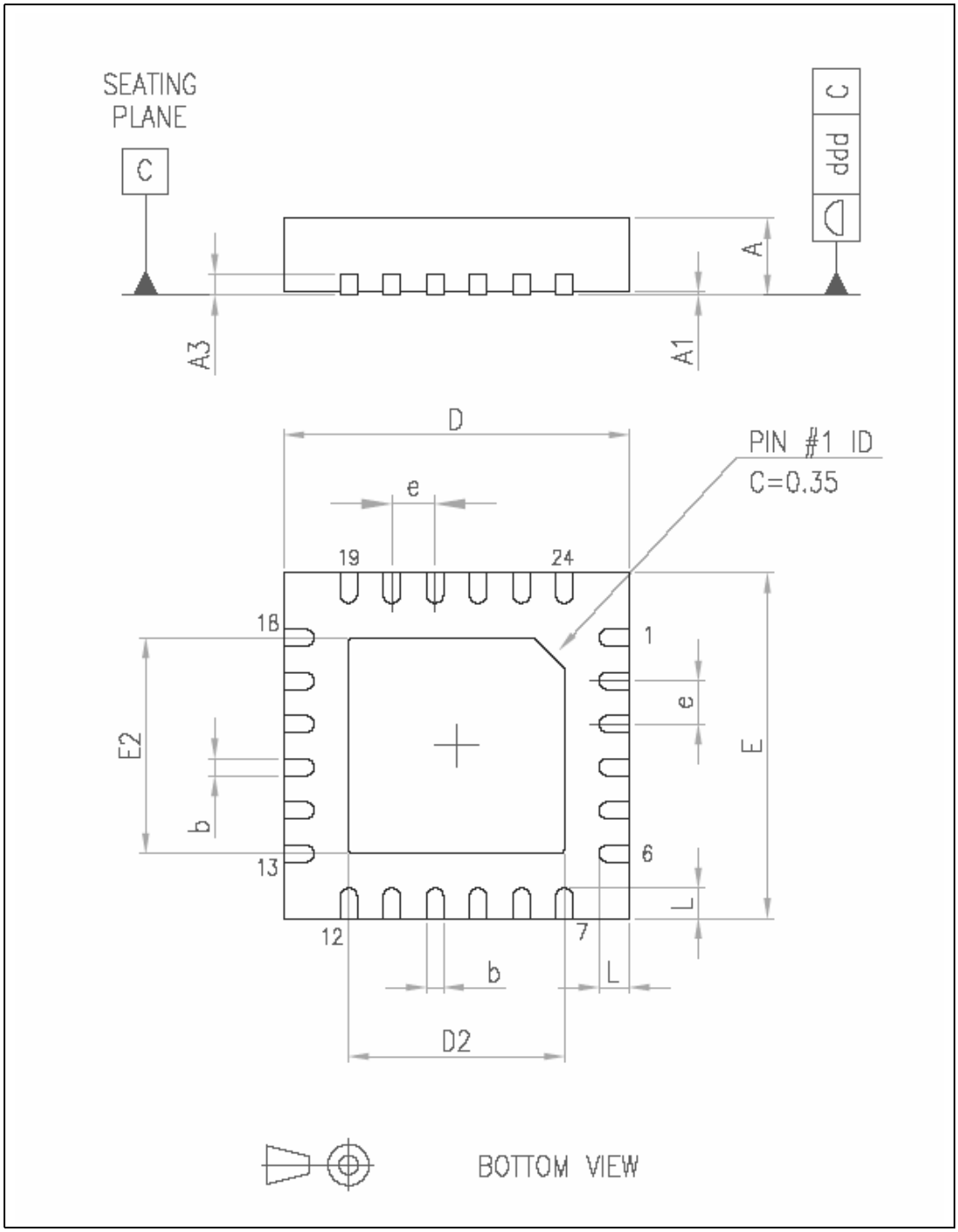

10 Revision history

Table 19. Document revision history

Date	Revision	Changes
14-Feb-2008	1	Initial release

Please Read Carefully:

Information in this document is provided solely in connection with ST products. STMicroelectronics NV and its subsidiaries (“ST”) reserve the right to make changes, corrections, modifications or improvements, to this document, and the products and services described herein at any time, without notice.

All ST products are sold pursuant to ST’s terms and conditions of sale.

Purchasers are solely responsible for the choice, selection and use of the ST products and services described herein, and ST assumes no liability whatsoever relating to the choice, selection or use of the ST products and services described herein.

No license, express or implied, by estoppel or otherwise, to any intellectual property rights is granted under this document. If any part of this document refers to any third party products or services it shall not be deemed a license grant by ST for the use of such third party products or services, or any intellectual property contained therein or considered as a warranty covering the use in any manner whatsoever of such third party products or services or any intellectual property contained therein.

UNLESS OTHERWISE SET FORTH IN ST’S TERMS AND CONDITIONS OF SALE ST DISCLAIMS ANY EXPRESS OR IMPLIED WARRANTY WITH RESPECT TO THE USE AND/OR SALE OF ST PRODUCTS INCLUDING WITHOUT LIMITATION IMPLIED WARRANTIES OF MERCHANTABILITY, FITNESS FOR A PARTICULAR PURPOSE (AND THEIR EQUIVALENTS UNDER THE LAWS OF ANY JURISDICTION), OR INFRINGEMENT OF ANY PATENT, COPYRIGHT OR OTHER INTELLECTUAL PROPERTY RIGHT.

UNLESS EXPRESSLY APPROVED IN WRITING BY AN AUTHORIZED ST REPRESENTATIVE, ST PRODUCTS ARE NOT RECOMMENDED, AUTHORIZED OR WARRANTED FOR USE IN MILITARY, AIR CRAFT, SPACE, LIFE SAVING, OR LIFE SUSTAINING APPLICATIONS, NOR IN PRODUCTS OR SYSTEMS WHERE FAILURE OR MALFUNCTION MAY RESULT IN PERSONAL INJURY, DEATH, OR SEVERE PROPERTY OR ENVIRONMENTAL DAMAGE. ST PRODUCTS WHICH ARE NOT SPECIFIED AS "AUTOMOTIVE GRADE" MAY ONLY BE USED IN AUTOMOTIVE APPLICATIONS AT USER’S OWN RISK.

Resale of ST products with provisions different from the statements and/or technical features set forth in this document shall immediately void any warranty granted by ST for the ST product or service described herein and shall not create or extend in any manner whatsoever, any liability of ST.

ST and the ST logo are trademarks or registered trademarks of ST in various countries.

Information in this document supersedes and replaces all information previously supplied.

The ST logo is a registered trademark of STMicroelectronics. All other names are the property of their respective owners.

STMicroelectronics group of companies

Australia - Belgium - Brazil - Canada - China - Czech Republic - Finland - France - Germany - Hong Kong - India - Israel - Italy - Japan - Malaysia - Malta - Morocco - Singapore - Spain - Sweden - Switzerland - United Kingdom - United States of America

www.st.com